JDEU 1 (1), (2025), 39-67

JDEU Journal of Dynamics, Energy and Utility

REVIEW ARTICLE

An Example of Multidisciplinary Work in Aviation: Radome Design

Salman Murat Durukan [1], Yeşim Öz [1], Ahmet Kardaş [1], Tuğba Burcu Çakır [1], Ahmet İvenç [1], Nursev Erdoğan [2], Mustafa Kocaman [2], Mesut Uyaner [1*]

[1] Necmettin Erbakan Üniversitesi, Faculty of Aeronautics and Astronautics, Department of Aeronautical Engineering, Konya, TÜRKİYE
[2] TUSAŞ Turkish Aerospace Industries, Inc., Ankara, TÜRKİYE
*Corresponding Author *.* muyaner@erbakan.edu.tr

Received. 29.04.2025
Accepted. 25.05.2025

Abstract

Radome structures are essential in contemporary aerospace and defense systems, safeguarding radar equipment while facilitating the effective transmission of electromagnetic waves. This assessment offers a multidisciplinary analysis of radome design, concentrating on incorporating materials engineering, structural mechanics, aerodynamics, and electromagnetic efficiency. Particular focus is placed on composite materials featuring low dielectric constants, metamaterials, and frequency-selective surfaces (FSS), which enhance RF transparency and lower radar cross-section (RCS). The influence of structural shapes on aerodynamic resistance and high-speed mechanical strength is examined, along with typical failure modes due to environmental stressors like temperature changes, humidity, and UV radiation. Sophisticated numerical techniques like the Finite Element Method (FEM), Finite-Difference Time-Domain (FDTD), and Method of Moments (MoM) are examined for electromagnetic analysis. In contrast, Computational Fluid Dynamics (CFD) evaluates aerodynamic properties and flow dynamics. Furthermore, the document emphasizes recent advancements in combined optimization approaches and design software tools that concurrently tackle electromagnetic, mechanical, and aerodynamic needs. These methods encompass multidisciplinary design optimization (MDO) frameworks, topology optimization, and design iterations supported by machine learning. By merging these viewpoints, the research provides a comprehensive strategy for radome design and seeks to facilitate the advancement of next-generation aerospace systems with superior performance, lower detectability, and increased structural durability.

Keywords. *Radome design, Electromagnetic performance, Multidisciplinary optimization, Frequency selective surface (FSS), Radar cross section (RCS), Stealth technology*

1. Introduction

This study presents a comprehensive review of radome design approaches, including material selection, structural configurations, geometrical effects, and electromagnetic performance criteria. In addition to summarizing established methodologies, this work brings forward an integrated, multidisciplinary design perspective that combines electromagnetic, structural, aerodynamic, and thermal considerations within a unified framework. While prior literature typically addresses these domains in isolation, this study emphasizes their interdependence and explores how multi-physics optimization techniques can be applied holistically to radome systems.

Moreover, the review highlights recent advancements in adaptive radome technologies, such as the incorporation of metamaterials, FSS, and conformal integration methods, which are gaining strategic importance in next-generation aerospace applications. By systematically evaluating computational modeling approaches (e.g., FEM, CFD, EM solvers), material-performance interactions, and geometry-based optimization strategies, this study not only identifies current limitations but also proposes future research directions.

Ultimately, this study aims to offer a technically grounded, application-oriented, and forward-looking synthesis that will support future design, development, and integration of radomes in supersonic aircraft platforms and AESA radar systems—areas where the literature remains fragmented and often lacks interdisciplinary continuity.

2. Radome Materials and Structural Design

2.1 Composite and Dielectric Materials

Radomes used in high-speed aerial vehicles and missile platforms are not only required to protect radar systems from external environmental conditions but also to ensure the effective transmission of electromagnetic waves. Therefore, the fundamental properties expected from radome materials include low dielectric constant (ε_r), low loss factor (tan δ), high mechanical strength, and environmental resistance. The type of material used in radome structures plays a critical role in determining both electromagnetic transparency and mechanical strength. In this context, radome materials are generally classified under two main categories, conventional materials and advanced materials.

2.1.1 Conventional materials

Among the conventional materials widely used in radome manufacturing, polymer matrix composites reinforced with fiber such as fiberglass, quartz, and Kevlar® stand out. Fiberglass is frequently preferred due to its low cost and favorable mechanical properties; however, its electromagnetic transparency may be limited at high frequencies. Traditional dielectric materials such as several types of fiberglass (E-glass, S-glass, D-glass), quartz glass, and Kevlar® fibers have been commonly utilized in radome production for a long time. [1]. Quartz glass provides stable electromagnetic transparency even at temperatures up to 1300 °C, owing not only to its low coefficient of thermal expansion (CTE) ($\sim 0.5\times10^{-6}$/°C), low density, and extremely low loss factor (tan δ < 0.0012), but also to its high purity and robust molecular structure. Composed entirely of covalently bonded SiO_2 in a solid amorphous network, quartz glass requires significant thermal energy to disrupt its atomic structure, which contributes to its exceptional thermal stability [1]. The material properties are shown in Table 1.

Table 1. Characteristics of fiber materials evaluated under room temperature conditions [1]

Material	Dielectric Permittivity	Loss Tangent	Elastic Modulus (GPa)	Tensile Strength (GPa)	Density (kg/m^3)
E-glass	6.3	0.003	73.5	3.5	2540
S-glass	5.1	0.0068	86.8	4.66	2490
D-glass	4	0.0026	52.5	2.45	2160
Kevlar 49	3.85	0.019	112.4	3.60	1440

Composite structures, which are frequently used in radome systems, are produced by combining resin and reinforcement fiber components in specific ratios and orientations. Epoxy-based resins are widely utilized in aerospace applications due to their low loss tangent (tan δ ~ 0.005) and high mechanical strength properties. For systems operating at higher temperatures, high-performance resin systems such as polyimide and cyanate ester are preferred [2]. The dielectric properties of composite structures are influenced by several factors, including fiber orientation, interfacial interactions, and moisture absorption. Water absorption leads to undesirable increases in the dielectric constant and reductions in the glass transition temperature (T_g), which adversely affect both electromagnetic and mechanical performance [1].

Moreover, multilayer (sandwich) composite configurations, formed by combining a low-density core material with high-strength outer layers, provide significant advantages in terms of structural integrity and dielectric transparency. These structures offer ideal solutions, especially for multi-band radar systems [1].

2.1.2 Advanced materials

Advanced material technologies are extensively applied in radome systems to enhance electromagnetic performance. Within this scope, metamaterials—comprising sub-wavelength-scale resonators, as illustrated in Figure 1—enable the artificial realization of targeted transmittance and permeability characteristics [3].

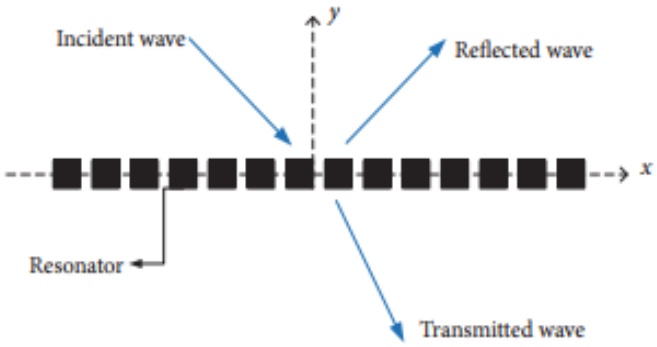

Figure 1. A Metasheet (metafilm) of arbitrarily shaped resonators arranged periodically in the x-y plane [3]

Metasheet structures offer the capability to control the transmission, reflection, and phase characteristics of electromagnetic waves through surface effects, thereby enabling low-loss and directional transparency. Planar structures designed based on Huygens' principle can perform the functions of conventional lenses in a compact form [2].

Reported designs in the literature demonstrate that significant improvements have been achieved in parameters such as gain enhancement, directivity improvement, and bandwidth expansion through appropriate element geometry and multilayering techniques [2].

2.1.3 Effects on electromagnetic and mechanical performance

The selection of materials used in radome structures is based on a delicate balance between electromagnetic transparency and structural strength. Especially in supersonic platforms, radomes are expected to provide high transmission at radar frequencies while withstanding severe aerodynamic and thermal loads [4]. Composite materials have been developed to meet these multidisciplinary requirements and are preferred due to their low density, high tensile and flexural strength, and low dielectric loss properties against radar waves [1]. A typical Type-A sandwich structure as shown in Figure 2, consisting of two high-density outer layers and a low-density core, is capable of simultaneously meeting both electromagnetic and mechanical performance criteria [5].

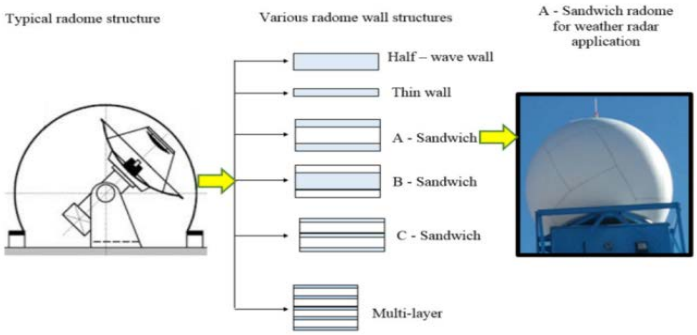

Figure 2. Common radome wall varieties utilized in radomes [5]

Glass fiber-reinforced polyester composites are frequently preferred in radome applications due to their low dielectric constants (3.0–3.5) and favorable wetting behavior. It has also been shown that increasing the glass fiber content significantly improves flexural strength and modulus. In specimens containing 15% boric acid and 20% fiber reinforcement, flexural strength reached up to 141.89 MPa [6].

Dielectric properties are directly related to the material's moisture absorption tendency and its structure, which varies with temperature and frequency. Water absorption increases the dielectric constant of composites, thereby deteriorating electromagnetic transparency; in addition, tensile strength losses of up to 24% have been reported in glass fiber-reinforced systems [1].

To enhance electromagnetic transmissivity in radome materials, parameters such as the thickness of material layers, dielectric constant values, and manufacturing conditions are optimized. In a study conducted at C-band frequencies, the surface layer had a dielectric constant of $\varepsilon_r \approx 3.15$, while the core layer measured around $\varepsilon_r \approx 1.05$ the total insertion loss was reported to be below 0.2 dB [5].

In this context, Table 2 [3] summarizes the key material properties to consider for electromagnetically and mechanically optimized radome materials.

Table 2. Common factors influencing radome effectiveness [3]

Mechanical	Electrical	Thermal	Environmental
Young's modulus	ε_r with temperature	Specific heat	Radiation exposure
Tensile strength	ε_r with frequency	Thermal conductivity	Rain erosion
Shear modulus	ε_r with humidity	Thermal shock resistance	Water absorption
Impact strength	tan δ with temperature	Thermal expansion	Chemical resistance
Fatigue	tan δ with frequency	Flammability	
Creep	tan δ with humidity		

For the reasons briefly outlined above, ensuring both electromagnetic transparency and long-term structural integrity in radome materials intended for use in high-speed aerial platforms requires an interdisciplinary optimization approach.

2.2 Structural Configurations and Geometric Effects

The geometric configuration of radomes has a significant impact on electromagnetic performance and aerodynamic behavior. Structural configurations not only ensure the protection of antenna systems but also directly influence direction-finding accuracy, gain performance, and transmission losses. Therefore, the appropriate selection of radome geometries requires a multidisciplinary optimization approach.

Radome geometry is a critical parameter that directly affects electromagnetic performance, structural strength, and aerodynamic drag. The shape of the radome determines key factors such as electromagnetic interaction with the antenna, boresight error, transmission loss, and frequency sensitivity [7], [8].

2.2.1 Types of radome geometry

Among the most common radome geometries are spherical, geodesic, ogival (von Kármán, tangent, secant), elliptical, conical, and Haack series profiles. Spherical radomes provide direction-independent transparency due to their isotropic structure; however, they may create aerodynamic disadvantages in high-speed applications. On the other hand, geodesic radomes offer advantages in large-scale systems with their panel-based structures, but they may cause phase distortions at the panel junctions [8].

According to the study by G. A. Crowell Sr., ogival geometries are particularly preferred in applications where aerodynamic requirements are prioritized. The tangent ogive represents a classical form with a circular arc profile tangentially connected to the body in Figure 3, while the secant ogive offers a more "bulged" structure that does not merge tangentially with the body [9].

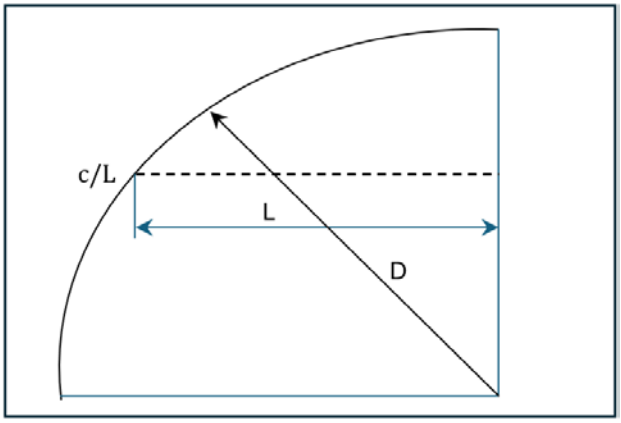

Figure 3. Geometry and parameters of the tangent ogive [9]

Elliptical geometries in Figure 4 are particularly preferred in subsonic speed applications due to their blunt nose shape and tangential body connection. However, compared to the von Kármán geometry, they generate higher wave drag [9].

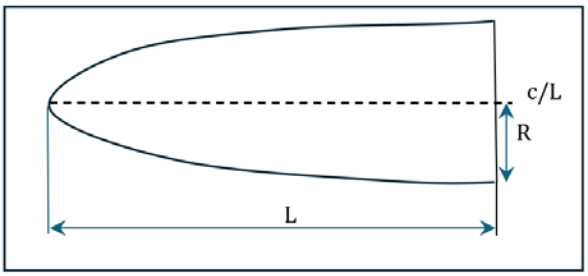

Figure 4. Elliptical nosecone geometry and parameters [9]

The Haack series, which can be considered an extension of the von Kármán geometry, has been derived based on aerodynamic optimization principles. The LD-Haack profile (C=0) is designed for minimum drag, while the LV-Haack profile (C=1/3) is based on the principle of minimum drag for a given volume. Although these forms may lead to certain deviations in terms of electromagnetic performance, they are widely preferred in high-speed platforms. The LV-Haack series is mathematically defined to provide minimum wave drag for a given length and diameter in Figure 5 [9].

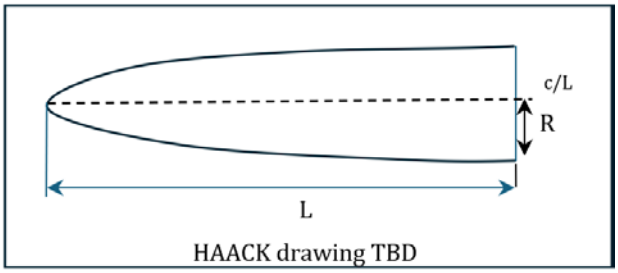

Figure 5. HAACK illustrating geometry and variables [9]

$$\theta = \cos^{-1}\left(1 - \frac{2x}{L}\right) \tag{1}$$

$$y = \frac{R\sqrt{\theta - \frac{\sin(2\theta)}{2} + C\sin\theta^3}}{\sqrt{\pi}} \tag{2}$$

$C = \frac{1}{3}$ for **LV-HAACK**

$C = 0$ for **LD-HAACK** (This is also known as the **von Kármán**, or the **von Kármán Ogive**)

Conical and bi-conical shapes are commonly used due to their manufacturing simplicity. However, these geometries generally exhibit high drag coefficients. The bi-conical structure is formed by the combination of two conical sections with different slopes and is utilized in adaptive transition regions [7].

2.2.2 Effect of thickness and curvature

Radome thickness has a direct impact on the reflection coefficient of electromagnetic waves. According to the "matched thickness" principle, the radome must be designed with an optimum thickness corresponding to a specific frequency. This approach minimizes transmission loss and phase deviation[5].

Curvature may lead to refraction and boresight errors, which affect the pointing accuracy of the antenna. This effect becomes particularly pronounced in ogival and hemispherical shapes as illustrated Figure 6. Since such geometries impact both electromagnetic transparency and aerodynamic performance, it is essential to address both disciplines simultaneously during the design process [3].

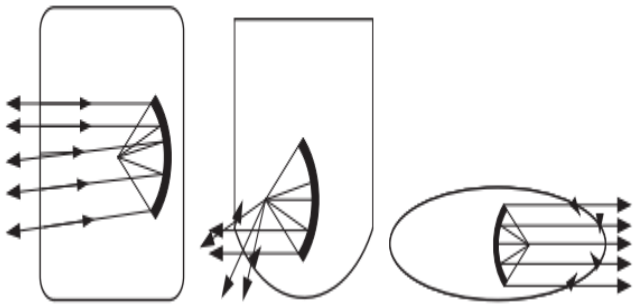

(a) (b) (c)

Figure 6. Varied shapes of radomes (a) cylindrical, (b) cylindrical-hemispherical, (c) spheroidal or ogival [3]

According to Öziş *et al.*, an increase in curvature ratio leads to a corresponding rise in boresight error, which should be compensated through electromagnetic correction techniques [3]. The influence of structural shapes on electromagnetic performance has also been experimentally validated. As illustrated in Figure 7, an increase in core thickness results in higher insertion loss while simultaneously reducing bandwidth and center frequency. In this figure, IL refers to insertion loss in decibels (dB), and h_{core} represents the core thickness in millimeters. Therefore, from an electromagnetic standpoint, thinner core layers are more favorable; however, structural requirements must also be taken into consideration [7].

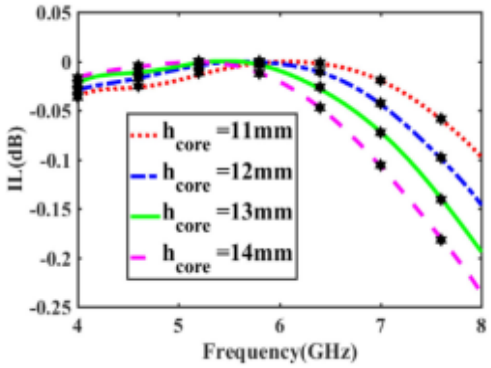

Figure 7. Impact of core thickness (h_{core}) on insertion loss (S_{21}) from 4 to 8 GHz [7]

The slope angle of the radome causes refraction within the beam path, leading to deviations in direction-finding accuracy. Therefore, in geometries such as the von Kármán type, it is recommended that angle-dependent refractions be pre-calculated using ray tracing analysis methods.

2.2.3 Structural types: monolithic and sandwich

Critical design parameters such as electromagnetic transparency and mechanical strength directly influence the selection of structural configurations in radome design. In this context, structural configurations are generally categorized into four main types. monolithic, A-sandwich, B-sandwich, and C-sandwich structures [10].

Monolithic structures consist of a single-layer, homogeneous dielectric material. These types of configurations are known to provide excellent electromagnetic transparency at reduced wall thickness. However, the mechanical strength tends to decrease with thinner walls, leading to insufficient structural integrity, especially under high external pressure conditions [10], [11].

Sandwich structures, on the other hand, typically comprise high-strength thin outer skin layers and a low-density core layer. A-sandwich structures consist of three layers (skin-core-skin), while C-sandwich structures include five or more layers and provide superior performance in terms of both broadband electromagnetic transmission and mechanical strength[10], [12].

For instance, in a study conducted by Özdemir et al., a comparison between A-sandwich (three-layer) and C-sandwich (five-layer) structures was carried out using finite element analysis. Although both structures withstood a hydrostatic pressure of 7.5 MPa, the C-sandwich configuration exhibited higher structural strength [10]. Figure 8 presents a visual comparison of these structural configurations.

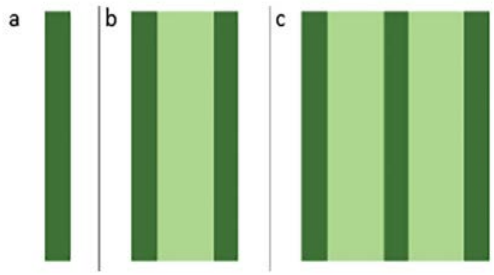

Figure 8. Radome wall designs include (a) monolithic, (b) a-sandwich, and (c) multilayered or c-sandwich configurations [10]

Sandwich structures also offer significant advantages in terms of electromagnetic performance. In A-sandwich structures, electromagnetic compatibility is achieved by selecting a low dielectric constant for the core material, while higher dielectric constant values are assigned to the skin layers. This configuration minimizes signal reflection and ensures better impedance matching between the radome and free space, thereby enhancing electromagnetic wave transmission. In analyses conducted on asymmetric A-sandwich structures, it has been demonstrated that by selecting different skin thicknesses and material types according to external and internal environmental conditions, transmission losses can be minimized [11].

In C-sandwich structures designed for high-frequency and multi-band applications, the optimum combination of core and skin layers can enhance both structural and electromagnetic performance. The multilayer C-sandwich radome design developed by Chepala et al. has been shown to successfully apply for dual-sensor systems operating in the 1–18 GHz and W-band frequency ranges [13]. Figure 9 presents the frequency transmission characteristics of the mentioned multi-band C-sandwich structure.

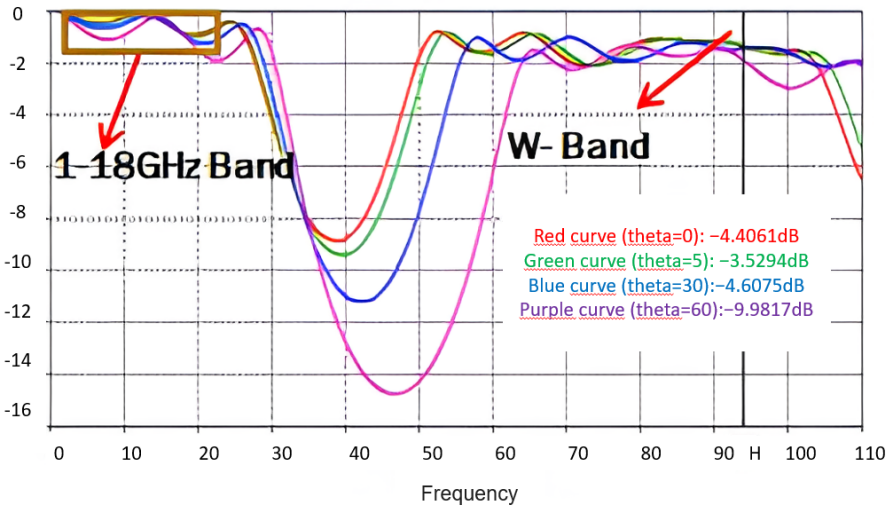

Figure 9. The C-sandwich radome frequency transmission graph [13]

3. Electromagnetic Performance and RF Transmission

3.1 Radome Design for Minimum RF Distortion

This section focuses on advanced radome design strategies developed to minimize radio frequency (RF) distortion, which is critical for maintaining the integrity of radar signals and ensuring high-performance electromagnetic transmission. Key considerations include the selection of materials with suitable dielectric properties, the optimization of structural geometry to reduce reflection and refraction effects, and the integration of technologies such as FSS and metamaterials. These approaches aim to preserve signal fidelity, reduce boresight error, and enhance the overall transparency and efficiency of the radome, particularly in high-speed aerospace applications. Furthermore,

the relationship between material selection, wave behavior, and backscatter has been extensively discussed in prior studies on radar RCS mechanisms [14].

3.1.1 The effect of radome materials on radar cross section

RCS is one of the most critical parameters that determine the target detection capability of radar systems. The RCS value indicates the number of electromagnetic waves sent by the radar that are reflected by the target. In this context, platforms with low RCS values are more difficult to detect by radar systems [14]. The materials used in the radome structure, geometric design, and surface properties directly affect the RCS value [15]. Due to the high reflectivity of metallic structures, these materials are generally not preferred in platforms where low observability is required [16].

Table 3 presents the dielectric constant and loss tangent values of polymeric radome materials used at 8.5 GHz frequency. In radome design, materials with a low dielectric constant and a low loss tangent are preferred to minimize transmission loss. According to Table 3, Teflon demonstrates the best electromagnetic performance among thermoplastic materials. With its low dielectric constant (2.10) and very low loss tangent (0.0005), it provides a high radar transparency. Similarly, Duroid 5650 stands out with its low characteristics.

In the laminate material group, Fiberglass laminate and Quartz-reinforced polyimide are balanced options in terms of both structural strength and electromagnetic performance. On the other hand, materials such as Epoxy E glass cloth have limited application areas due to their higher dielectric constant and loss tangent values.

Table 3. Polymeric materials for radomes at a frequency of 8.5 GHz [15]

Material	Dielectric Constant	Loss Tangent
Thermoplastic materials		
Lexan	2.86	0.006
Teflon	2.1	0.0005
Noryl	2.58	0.005
Kydox	3.44	0.008
Laminates		
Epoxy E glass cloth	4.4	0.016
Polyester-E glass cloth	4.1	0.015
Polyester-quartz cloth	3.7	0.007
Polybutadiene	3.83	0.015
Fiberglass laminate polybenzimidazole resin	4.9	0.008
Quartz-reinforced polyimide	3.2	0.008
Duroid 5650 (loaded Teflon)	2.65	0.003

Therefore, composite materials and radar-absorbing materials (RAM) are widely used in modern radome designs [16]. RAM applications reduce the level of reflected signals by enabling the absorption of electromagnetic waves on the radome surface, thereby decreasing the RCS value [16].

In addition, the performance of RAM materials depends on various parameters such as operating frequency, environmental durability, temperature tolerance, and mechanical strength. Geometric configuration also plays a critical role in RCS reduction. Surface designs such as ogive, conical, and paraboloid shapes help reduce radar visibility by scattering the incident electromagnetic waves in different directions depending on the angle of incidence [15].

Moreover, minimizing surface roughness, rounding sharp edges, and applying dielectric coatings to the structure are also considered effective strategies for reducing RCS.

3.1.2 Minimization of transmission loss and boresight error

Transmission loss occurs because of the energy loss of electromagnetic waves while passing through the radome, leading to a decrease in radar performance. This loss is associated with several parameters, including the material's dielectric constant, loss tangent, thickness, moisture absorption, and temperature variability [15]. Therefore, using materials with minimal loss becomes critical, especially at high frequencies. The use of low-loss dielectric materials is critical to enable nearly lossless wave propagation within the radome.

In radome design, multilayer structures are also applied to minimize phase shifts and diffraction effects. In the design of such structures, the thickness ratio between layers, material properties, and interface smoothness are essential parameters. Phase-correcting layers are employed to prevent the deflection of electromagnetic waves in the antenna direction and to minimize transmission loss [17].

Another significant parameter is Boresight Error (BSE), which refers to the deviation of the radar antenna's transmission direction. It is considered a critical problem, particularly in platforms requiring high-speed maneuverability [18]. In the studies conducted by Peterson et al., it has been indicated that minimizing BSE requires optimizing the distance between the antenna and the radome, maintaining a uniform radome wall thickness, and preserving electromagnetic symmetry [18]. In addition, minimizing structural manufacturing defects, ensuring material homogeneity, and balancing thermal expansion factors are also crucial for controlling BSE.

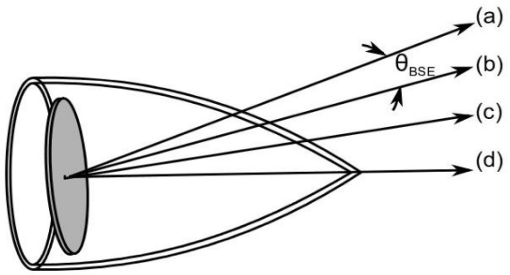

Figure 10. Illustration of boresight error (a) apparent line of sight (b) actual line of sight (c) antenna centerline (d) radome centerline [19]

Figure 10 conceptually illustrates BSE, a critical performance criterion in radome design. In radome-equipped systems, electromagnetic waves undergo refraction as they pass through the radome, resulting in a deviation between the actual line of sight of the antenna and the apparent line of sight emerging from the radome. This angular deviation is defined in the literature as a boresight error (BSE). Figure 10 illustrates the deviation in electromagnetic wave propagation due to the presence of a radome. The line marked (a) represents the apparent line-of-sight of the antenna when the radome is present, showing the refracted path of the signal. Line (b) indicates the actual line-of-sight of the antenna in the absence of a radome, which represents the true direction of the beam. Line (c) denotes the antenna centerline, reflecting the ideal transmission axis of the system, while line (d) shows the radome centreline, aligned with the geometrical axis of the radome shell. The angle Θ_{BSE} between lines (a) and (b) defines the angular boresight error, a critical parameter in radome performance, representing the angular deviation introduced by the radome material and shape. Here, Θ_{BSE} represents the angular deviation between the antenna and the radome.

The primary causes of BSE include the dielectric properties of the radome material, variations in wall thickness, surface curvature, and the lack of optimization in the distance between the radome and the antenna. In high-frequency radar systems, this error becomes significantly more pronounced and negatively affects target detection accuracy.

To minimize BSE in radome design, several fundamental strategies are employed. One prominent solution involves the use of phase-correcting layers to reduce diffraction and phase shifts of electromagnetic waves. Additionally, designing the radome wall with uniform thickness across all regions helps reduce electromagnetic anomalies and deviations. Maintaining consistent and controlled dielectric properties of the materials used is also a critical factor in preventing the formation of BSE. Finally, the proper alignment of the antenna and radome centerlines, along with the preservation of structural symmetry, ensures the correct transmission path of electromagnetic waves and minimizes BSE.

3.1.3 Adaptive radome designs with frequency selective surface

With the advancement of technology, FSS have gained significant importance in modern radome designs. FSS structures are defined as surfaces that allow electromagnetic wave transmission within specific frequency bands, while reflecting or absorbing unwanted frequencies [20]. This frequency selectivity primarily arises from the periodic geometry and resonant behavior of the unit cells, which are designed to interact constructively or destructively with specific electromagnetic wavelengths. In this way, radar performance is optimized while ensuring low observability against enemy radar systems. This approach naturally brings attention to various structural characteristics that must be carefully considered to achieve both optimal transmission and effective shielding. Through the optimization of these parameters, both the transmission loss of the radome is reduced and improvements in RCS performance are achieved. Furthermore, due to their multi-band operation capability, wide-angle performance, and adaptability to different electromagnetic conditions, FSS structures are widely used in adaptive radome designs [17]. One of the most important advantages of FSS structures is their low manufacturing tolerance and lightweight characteristics. These structures, which can be easily integrated into conformal surfaces, offer several benefits in modern aerial platforms, such as enhanced performance, durability, and low radar visibility [20].

3.2 Numerical Simulations and Computational Modeling

In radome design, electromagnetic transmission characteristics, structural strength, and the effects of aerodynamic loads are evaluated together within a multidisciplinary analysis process. In this context, based on the radiation characteristics obtained from antenna modeling, far-field predictions are carried out, and the effects of the radome on antenna performance are analyzed, particularly in terms of boresight error and sidelobe levels. Subsequently, the frequency-dependent transmission loss values of the radome wall structure are examined, and the electromagnetic transmission performance is evaluated. In the structural analysis phase, potential damage scenarios — particularly against impact loads such as bird strikes — are modeled, and the resulting deformation and stress distributions on the radome are assessed.

In the final stage, aerodynamic loads acting on the radome surface are determined using CFD (Computational Fluid Dynamics) analyses, and these are evaluated together with the deformation data obtained from the structural analysis to comprehensively assess the overall performance of the design. This sequence is clearly illustrated in Figure 11.

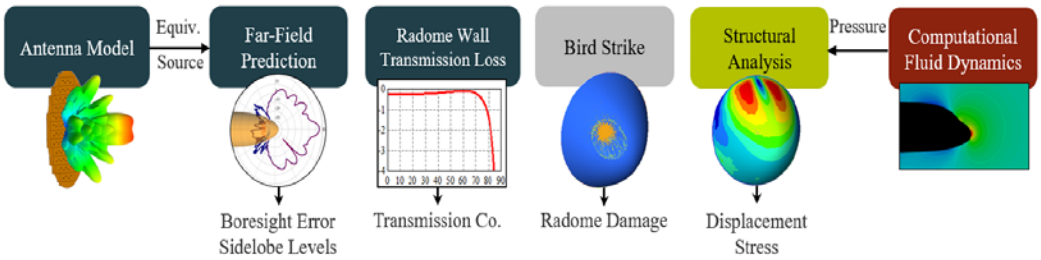

Figure 11. Cross-disciplinary assessment procedure examining the electromagnetic, structural, and aerodynamic efficiency of the radome [21]

3.2.1 Electromagnetic simulations (FEM, FDTD, MoM methods)

Electromagnetic (EM) simulation techniques are among the essential tools in modern radome design for analyzing and optimizing antenna–radome interactions. In this context, computational electromagnetic analysis methods such as the Finite Element Method (FEM), Finite-Difference Time-Domain (FDTD), and Method of Moments (MoM) are widely used to model the behavior of systems operating across various frequency bands. FEM is particularly preferred for the detailed analysis of complex geometries and material inhomogeneities. With its ability to accurately resolve three-dimensional geometrical details, this method effectively reveals the effects of frequency-dependent losses and variations in electrical thickness [22]. The FDTD method, operating in the time domain, plays an effective role in broadband analyses and the examination of transient behavior [23]. MoM-based approaches provide efficient solutions, especially for planar or multilayered structures. For example, the layered structures of radome walls can be analyzed using MoM through planar Green's functions to predict transmission losses [21]. Although the classical MoM requires intensive computational resources, this requirement has been significantly reduced using Fast Multipole and Multilevel Fast Multipole Methods [23]. Ray-launching techniques and physical optics methods are also commonly applied to aerodynamically shaped large radome surfaces. Using geometric optics-based 3D ray-tracing algorithms developed by Nair *et al.*, EM transmission behavior on curved surfaces has been modeled with high accuracy [22].

All these methods enable accurate prediction of key performance parameters of the antenna–radome system, such as boresight error, transmission coefficient, and cross-polarization levels.

3.2.2 Experimental validation methods of RF performance

As a complement to numerical analyses, experimental characterization methods are widely employed to validate the electromagnetic performance of radomes under real operating conditions. In this context, critical parameters such as transmission loss, boresight error, and sidelobe behavior are measured. One commonly used approach is to determine the transmission characteristics of the radome wall structure against plane waves at different angles of incidence using the planar Green's function method. This technique often utilizes systems integrated with frequency-swept Vector Network Analyzers (VNAs) [21]. To evaluate the radiation patterns of full-scale radomes in space, far-field test setups are established, and the performance of the antenna–radome system under free-space conditions is assessed. These tests are based on co-modeling the antenna and radome, and validation is achieved by comparing experimental results with simulation data obtained from numerical methods such as the Method of Moments (MoM) or Ray Launching Geometrical Optics (RL-GO) [21]. Additionally, by analyzing the radome's response to electromagnetic waves arriving from various angles, boresight error can be estimated. Studies have reported that angular deviations below 1° fall within the resolution limits of the measurement system, indicating that the designs achieve sufficient accuracy. During the experimental validation process, particular emphasis is placed on the measurement of transmission (S21) and reflection (S11) coefficients. For this purpose, rotary table systems integrated with VNAs are used to perform measurements at different angles of incidence and polarizations [10]. An example of such an experimental setup is shown in Figure 12.

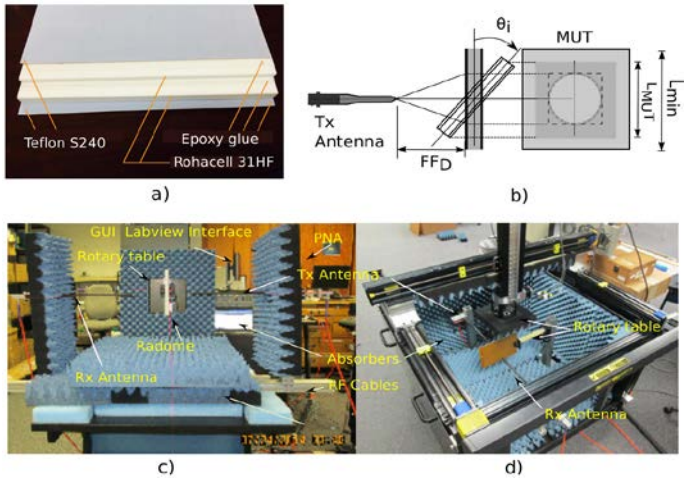

Figure 12. Radome materials under test and experimental setups: (a) A-sandwich panel consisting of Teflon S240 skins and Rohacell 31HF core bonded with epoxy glue, (b) schematic representation of the transmit antenna and the MUT, (c) open-space RF scanner with GUI-controlled rotary table, and (d) improved measurement setup with metallic enclosure for reduced environmental reflections [10]

In addition, the environmental durability of radome materials is also experimentally tested. Characterization studies conducted under wet surface conditions have compared hydrophobic and superhydrophobic coatings, revealing that the Hirec 100 coating demonstrates superior performance in terms of water repellency [10]. For the detection of possible structural defects in radome structures, Non-Destructive Evaluation (NDE) methods are commonly employed. Especially in systems incorporating FSS, the Inverse Source Reconstruction (ISR) technique has been reported to provide effective results in detecting metallic defects and displacements [24].

In conclusion, supporting the data obtained from numerical modeling methods with experimental techniques enables a comprehensive evaluation of the electromagnetic and structural performance of radomes. In this way, design accuracy is enhanced, while significant advantages are provided in terms of cost and time efficiency.

4. Aerodynamic And Structural Analysis

4.1 Aerodynamic Factors in Radome Design

Radome design is directly related not only to electromagnetic transparency but also to aerodynamic performance. In this context, radome geometry is one of the most critical parameters affecting aerodynamic drag and, consequently, flight stability. The optimization of radome shape is of vital importance to reduce aerodynamic loads encountered during flight, minimize fuel consumption, and maintain the maneuverability of the platform [25]. Figure 13 shows a comparison of radome geometries. From an electromagnetic perspective, an L/D ratio of approximately 1/2, representing a hemispherical shape, is considered ideal as it minimizes boresight error, signal phase distortion, and transmission loss. Conversely, an L/D ratio of approximately 5, corresponding to a long, slender shape, is aerodynamically advantageous. This is due to the minimization of drag, delays in flow separation, and support for smooth airflow over the surface, which is critical for high-speed flight regimes such as supersonic or hypersonic conditions. In conclusion, while an L/D ratio of 1/2 optimizes electromagnetic transparency and signal integrity, an L/D of 5 enhances aerodynamic efficiency for high-speed flight.

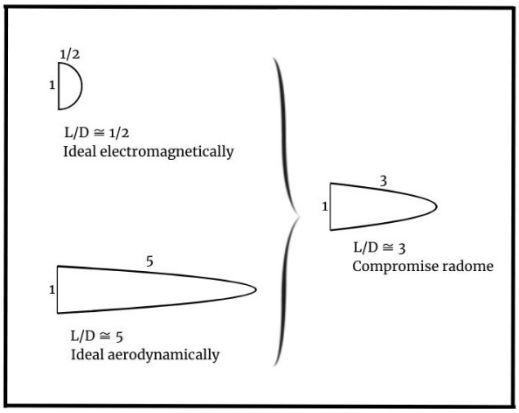

Figure 13. Analysis of radome shapes developed according to varying performance criteria [25]

4.1.1 Effects of radome geometry on aerodynamic drag and flight stability

In the study conducted by Varma *et al.*, it was demonstrated that boundary layer separation can be delayed by optimizing the nose shape of the missile [26]. The key approach highlighted in the study suggests that the static pressure at the base of the forebody should be increased as much as possible. In this way, it is indicated that the critical Mach number can be maximized, and the adverse pressure gradient formed on the cylindrical afterbody can be minimized. Although it is stated that vortex formation cannot be eliminated, it is emphasized that the effects of these vortices can be reduced by selecting an appropriate nose cone geometry. It has been shown that geometries capable of achieving high critical Mach numbers generate higher pressure coefficients (Cp) compared to ambient pressure. It was concluded that the closer the local minimum value of Cp is to zero, the weaker the adverse pressure gradient becomes, resulting in lower vortex-induced forces [27]. In the von Kármán ogive profile, the gradual acceleration of the flow leads to a higher critical Mach number. The von Kármán ogive nose profile is preferred in subsonic flows due to its desirable characteristics of achieving high critical Mach numbers and minimizing the pressure coefficient [27].

4.1.2 Flow analysis with computational fluid dynamics (CFD) simulations

Mesh convergence is a crucial step in CFD (Computational Fluid Dynamics) analysis. It involves increasing the number of mesh cells in the simulation until the solution values of the relevant variables converge to a stable value. The results of CFD analysis are essential for evaluating the aerodynamic performance of a radome structure. The analysis reveals that the drag coefficient and drag force on an elliptically shaped radome remain extremely low, even at maximum velocity and angle of attack. A low drag coefficient indicates that the radome structure is more aerodynamic and offers less resistance to fluid flow. Moreover, a low drag force minimizes the aerodynamic loads on the radome and the aircraft, thereby enhancing the overall performance [28]. A three-dimensional CFD analysis was used to calculate the aero pressure loads on the radome under various flight conditions. For CFD simulations, only the front half of the body was modeled, since full-vehicle CFD models are computationally expensive [28]. Considering the antenna size and the aerodynamic regime of the radome, an elliptical radome shape was selected because it provides minimum drag at subsonic speeds [28].

In the study conducted by Charan *et al.*, the aerodynamic effects experienced by different radome geometries at supersonic speeds (Mach 3) were analyzed using the CFD method [25]. The simulation results showed that the elliptical-shaped radome had the lowest drag coefficient, making it the most advantageous option in terms of aerodynamic efficiency under supersonic flight conditions. Contour analyses of pressure, temperature, and velocity distributions also revealed that the elliptical shape exhibited the lowest resistance to airflow and provided a more streamlined profile [25]. In this context, it was concluded that CFD analyses can serve as a guiding tool in the search for optimum nose designs.

In another study conducted by L. de A. S. Carvalho and G. C. C. Filho, the drag forces experienced by different nose cone geometries within the subsonic speed range (Mach 0.05–0.62) were comparatively analyzed using CFD methods [27]. The elliptical, parabolic, tangent, and conical nose profiles used in the simulations were evaluated under standard atmospheric conditions. The results indicated that the elliptical nose shape had the lowest average drag value at low speeds. The findings demonstrated that the effect of nose geometry on drag force varies depending on the velocity regime [27].

4.2 Mechanical Strength and Damage Mechanisms

In radome systems, mechanical strength is critically important not only for structural safety but also for ensuring the continuity of electromagnetic performance. Therefore, it is essential to investigate in detail the damage mechanisms that may occur under high-speed conditions, environmental effects, and impact-like loads. This section considers the literature and presents the fundamental damage modes

observed in radome structures, stress accumulations caused by environmental factors, and the reflections of these effects on radome performance.

4.2.1 Stress and load distribution under high-speed conditions

Under high-speed flight conditions (Mach 2 and above), pressure loads on the aerodynamic surface of the radome and thermally induced expansions due to heat result in localized stress accumulations. These stresses can trigger damage modes such as cracking and delamination, particularly at the edges and connection points of the structure. When composite sandwich structures are used, the elastic modulus of the core material and the shear strength of the surface layers play a critical role in withstanding these loads [29]. Indeed, Figure 14 illustrates the influence of the local coordinate system on the radome in the context of shell geometry and load directions.

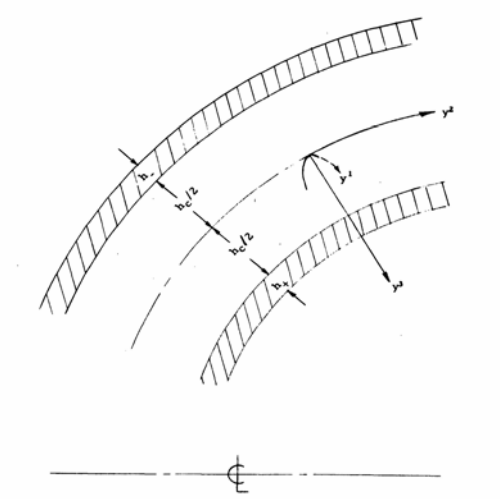

Figure 14. Shell structure and local reference frame [29]

Numerical analysis studies have shown that five-layered C-sandwich structures provide higher stress and deformation resistance compared to conventional three-layered A-sandwich structures [10]. It has been determined that these structures exhibit greater stiffness under axial loading conditions and possess higher energy absorption capacity during impact events. Figure 15 presents a detailed view of the stress distribution observed on these structures, while Table 1 provides a comparative summary of the mechanical properties of different sandwich configurations.

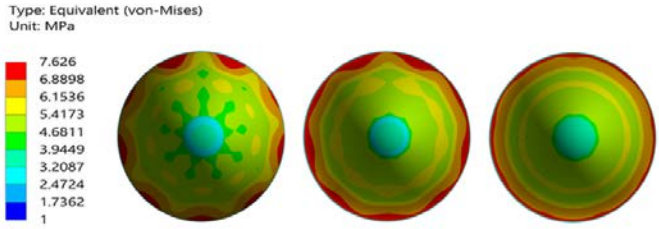

Figure 15. Stress allocation in sandwich composite structure [10]

4.2.2 Resistance to environmental factors

When radome materials are exposed to external environmental conditions, factors such as moisture absorption, temperature variation, UV radiation, rain erosion, and ice loads can adversely affect the electromagnetic and mechanical properties of the structure. Moisture absorption in polymer matrix composites leads to plasticization of the matrix and loss of adhesion at the interfaces, which accelerates crack formation [24]. This phenomenon has been observed through the changes in the parameters presented in Table 4.

Table 4. Physical characteristics (weight, elasticity modulus, etc.) [2]

Materials/Properties	Alumina	Pyroceram	Slip Cast Fused Silica	Cordierite Rayceram	Boron Nitride (Dense)	Silicon Nitride (Dense)	Silicon Nitride (RB)
Density (gm/cc)	3.9	2.6	2.2	2.45	2	3.2	2.4
Dielectric constant @10GHz, 25C 500C 1000C	9.6 10.3 11.4	5.65 5.8 6.1	3.42 5.8 3.8	4.85 5.05	4.5 4.6 4.78	7.9 8.2	5.6 5.7 5.8
Loss tangent @10GHz, 25C 500C 1000C	0.0001 0.0005	0.0002 0.001	0.0004 0.00	0.002 0.008	0.0003 0.0006	0.004 0.0045	0.0010 0.0025
Flexural Strength (MPa) 25C 500C 1000C	270 250 285	235 200 75	44 54 66	125 120	100 60	400 400	- -
Young Modulus (MPa) 25C 500C 1000C	 380 250 285	 120 120 100	 48 48 -	 128 125 120	 70 50 -	 300 300 -	 - - -
Thermal conductivity 10 GHz (W/ (m.K)) 25C	37	3.75	0.8	2.51	20.9	25.1	-
TCE (10^{-6} cm/degC)	8.1	4	0.54	2.3	3.2	3.2	-
Bending strength (MPa)	-	155	0.027	-	-	137	400
Thermal shock	Fair	Good	Very Good	Good	Very Good	Very Good	Very Good
Water absorption	0%	0%	5%	0%	-	-	20%
Rain erosion	Excellent	Very Good	Poor	Very Good	Very Good	Very Good	Good

Ceramic-based materials offer greater resistance to environmental variations due to their thermal stability and low coefficient of thermal expansion. Alumina and Pyros ceramics can largely maintain their dielectric constants even at temperatures exceeding 1000 °C, making them suitable solutions for high-speed platforms [2].

On the other hand, in polymer matrix composite structures, deformations caused by moisture absorption and temperature fluctuations represent a significant structural risk. Figure 16 illustrates the minimum principal stress distribution in the MCoRDS radome design for two different material configurations. Subfigure (a) represents the prepreg S2-glass/epoxy composite, while subfigure (b) shows the quartz-based design using experimentally measured properties. Both configurations demonstrate a similar overall stress distribution pattern; however, the key difference lies in the stress magnitude. The quartz-based design reduced approximately 900 psi in peak minimum principal stress compared to the prepreg design. This indicates that the quartz configuration, with its tested mechanical properties, offers improved structural performance under identical loading conditions [24].

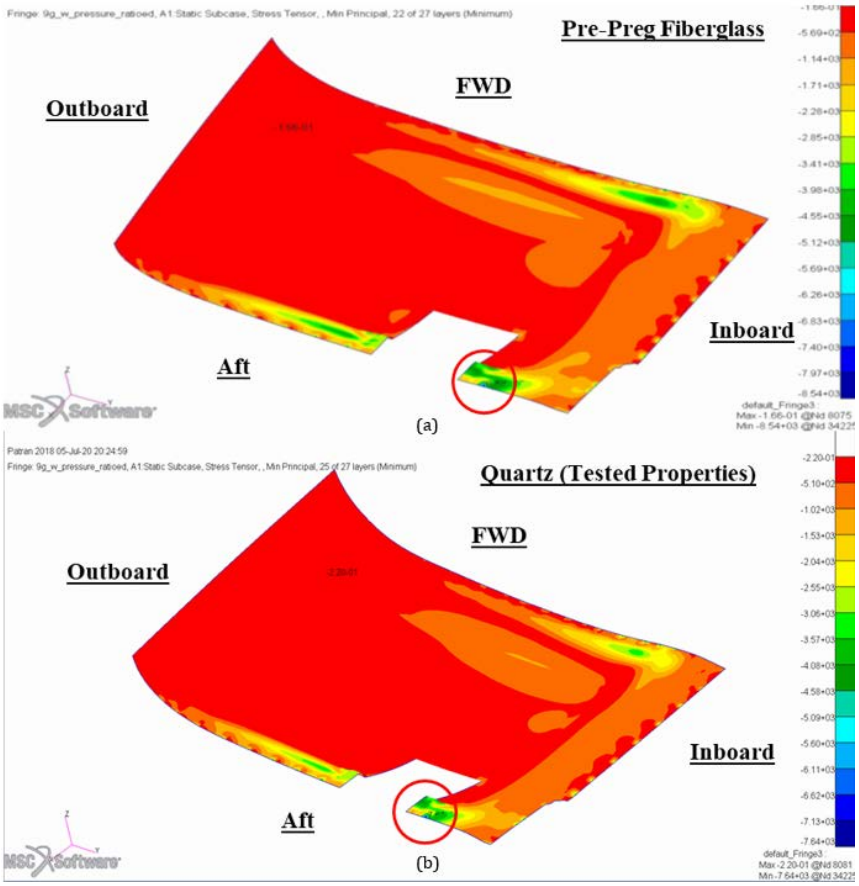

Figure 16. Minimum principal stress distribution in mcrds dielectric radome under simulated pressure loading: (a) prepreg fiberglass material configuration, (b) Quartz-based radome using experimentally obtained material properties [24]

4.2.3 Damage mechanisms

The most common damage mechanisms observed in radome structures include interlaminar delamination, core crushing, surface cracking, and fiber breakage. These damage modes are generally classified as Mode I (opening), Mode II (shear), and Mode III (tearing) fracture modes. Experimental studies have reported that Mode I and Mode II fracture mechanisms absorb more energy; therefore, progressive fracture behaviors are considered preferable damage patterns in terms of structural integrity and energy dissipation [30].

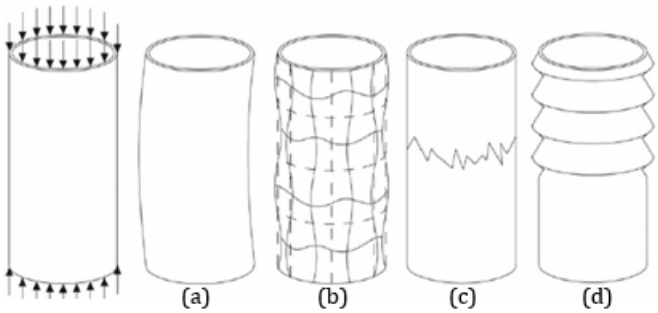

Figure 17. Failure mode on axial compression: (a) global buckling, (b) local buckling, (c) fracture, and (d) progressive crushing [31]

In their studies on composite tubes with different geometries and fiber orientations, Lau *et al.* demonstrated that shape factors — such as cone angle and cross-sectional form — significantly influence both the type of damage and the energy absorption capacity [31]. It was determined that round cross-sections and edge-triggered structures exhibit a more stable fracture mode and provide higher specific energy absorption than square cross-sections. Figure 17 illustrates the effect of different cross-sectional geometries on deformation modes.

5. Multidisciplinary Optimization and Design Software

5.1 The Importance of Multidisciplinary Optimization

The term "radome" is derived from the combination of "radar" and "dome" [32], and its primary function is to provide a protective cover between the antenna and the external environment while minimizing the impact on the antenna's electrical performance [33]. Factors such as aerodynamic loads encountered at high speeds, thermal stresses, and mechanical strength directly influence radomes' material and geometry selection. The requirements of different engineering disciplines, which often conflict with one another, increase the complexity of radome design.

From an electromagnetic perspective, radome design should be carried out to minimize the adverse effects on antenna performance. Ideally, the radome should be electrically transparent and have minimal impact on the transmission of electromagnetic waves. From an aerodynamic standpoint, the radome structure must feature streamlined shapes optimized to achieve low drag forces. Radomes must enable effective transmission of electromagnetic waves while protecting radar systems from external factors and maintaining structural integrity at high speeds, thus ensuring aerodynamic efficiency [34].

Parameters such as electromagnetic transparency, structural integrity, and aerodynamic efficiency must be evaluated using a multidisciplinary approach to achieve optimum performance, and an integrated optimization process must be adopted to balance design requirements effectively.

Radome design is inherently a multidisciplinary process in which different engineering fields are interrelated. The multidisciplinary requirements in radome design have rendered conventional single-discipline optimization techniques inadequate to meet the increasing complexity. Therefore, simulation-based Multidisciplinary Design Optimization (MDO) approaches — capable of addressing electromagnetic, structural, and aerodynamic parameters in an integrated manner — are becoming increasingly critical. These methods accelerate the design process and enable the development of higher-performance and cost-effective solutions.

Traditional design approaches generally divide this process into sequential phases. The mechanical responses are reviewed after completing the electromagnetic (EM) evaluation of the radome design. If structural requirements are not sufficiently met, the design process may return to its initial phase. This situation leads to a time-consuming and costly process to achieve the final design.

Previous studies have primarily focused on radomes' electromagnetic performance or mechanical strength, and these two factors have often been treated independently [34]. Simulation techniques for analyzing the electromagnetic properties of radomes have been well developed and generally classified into high-frequency and low-frequency methods [35]. High-frequency methods include Geometrical Optics (GO)-based Ray Tracing (RT), Physical Optics (PO)-based Aperture Integration–Surface Integration (AI-SI), and Plane Wave Spectrum–Surface Integration (PWS-SI). In contrast, low-frequency methods prominently feature the Finite Element Method and the Method of Moments (MoM) [35]. However, these techniques have neglected mainly mechanical properties and thermal effects, with optimization efforts limited to adjusting dielectric properties and basic geometric shaping.

Since the 2000s, researchers have started incorporating structural and mechanical parameters into radome optimization. The increased use of composite materials in radome design has necessitated the evaluation of mechanical strength, impact resistance, and thermal durability. During this period, Finite Element Analysis for structural assessment and CFD for aerodynamic analyses have become widely used. Research has particularly focused on sandwich radome structures, aiming to optimize core and skin thickness to ensure electromagnetic transparency and structural durability.

5.2 Multidisciplinary Optimization Methods and Software Tools

In traditional radome designs, engineering disciplines have generally been addressed independently, and each parameter has been optimized separately. However, the increasing complexity of modern radome designs and the importance of interdisciplinary interaction have demonstrated that these independent analyses are no longer sufficient. In this context, multidisciplinary optimization methods, which consider the interaction between different disciplines, enable the development of more efficient and practical designs. The interdisciplinary design approach ensures that complex engineering problems are addressed holistically by integrating expertise from various engineering disciplines. With this approach, interdependent design criteria, such as electromagnetic performance and structural stability, can be optimized simultaneously. Particularly in the design of sandwich-structured radomes, all physical factors affecting the radome’s performance can be evaluated collectively through the collaboration of disciplines such as electromagnetics, structural analysis, material science, and thermal analysis [34]. This interdisciplinary interaction not only increases design accuracy but also allows the emergence of innovative solutions that conventional single-discipline methods might overlook.

This section will discuss the multidisciplinary optimization methods used in radome designs, current MDO principles, and interdisciplinary design software tools.

5.2.1 Multidisciplinary optimization methods

Multidisciplinary optimization methods used in radome designs represent a process in which different engineering disciplines (such as electromagnetics, structural analysis, aerodynamics, etc.) are addressed together, and design parameters are optimized while considering their interactions. The entire design process is optimized by considering each discipline's specific requirements and constraints.

5.2.1.1 Multidisciplinary design optimization (MDO)

Multidisciplinary Design Optimization is an engineering field that employs optimization methods to solve design problems involving multiple disciplines. It is also referred to as Multidisciplinary System Design Optimization (MSDO) or Multidisciplinary Design Analysis and Optimization (MDAO) [36]. This approach lets designers evaluate all relevant domains simultaneously, offering a holistic solution rather than optimizing each discipline separately. By leveraging interdisciplinary interactions, more efficient and effective outcomes can be achieved. Figure 18 schematically presents the role of MDO in complex engineering design and product development processes. In such design processes that require concurrently operating multiple disciplines, MDO tools enhance efficiency through design space exploration, decomposition, simulation modeling, sensitivity analysis, and information flow management.

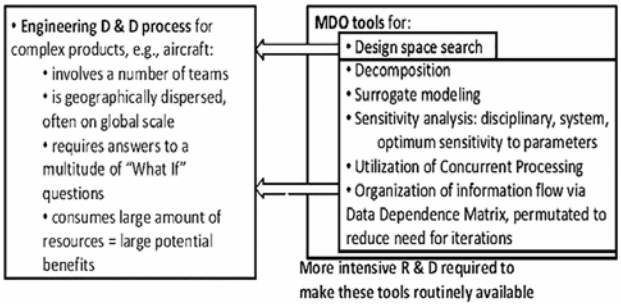

Figure 18. MDO in engineering design and product development [37]

5.2.1.2 MROS (multidisciplinary radome optimization)

Multidisciplinary Radome Optimization is a specialized multidisciplinary optimization system explicitly developed for radome design, and it can be considered a particular subset of the broader MDO framework. However, the primary focus of MROS is to provide optimized solutions to enhance the durability and reliability of radome structures. With the implementation of MROS, integrated analyses that simultaneously account for electromagnetic, mechanical, thermal, and aerodynamic performance have become feasible. MROS enables the optimization of design parameters in line with multiple objective functions by considering the interactions between different engineering disciplines throughout the design process. From the electromagnetic perspective, it incorporates algorithms designed to minimize boresight error and phase distortion, while in structural analysis, it evaluates the behavior of the radome under mechanical loads.

Today, advanced simulation tools such as HFSS (for electromagnetic analysis), ANSYS ACP (for composite structural design), and CFD solvers (for aerodynamic analysis) are utilized in integrated workflows within MROS frameworks.

5.2.1.3 Metaheuristic algorithms

Metaheuristic algorithms are general-purpose algorithms inspired by natural processes and are used to solve complex optimization problems. These algorithms are particularly preferred in scenarios where classical optimization methods are inadequate, such as in nonlinear, multi-objective, constrained issues or problems with large spaces. The literature includes more than 300 metaheuristic algorithms [38]. As illustrated in Figure 19, these algorithms can be classified based on their underlying inspiration mechanisms into various categories, including physics-based, biology-based, chemistry-based, mathematics-based, swarm-based, social, music-based, sports-based, plant-based, water-based, and hybrid approaches [39].

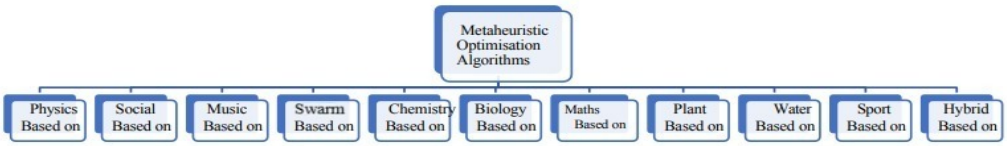

Figure 19. Classification of Metaheuristic Optimization Techniques [39]

5.2.1.3.1 Genetic algorithm (GA)

The Genetic Algorithm is a heuristic search technique used to find the optimal solution to a problem, inspired by the processes of natural evolution. Holland first established the theoretical foundations of GA in 1975 [40]. GA operates through a series of steps, including the generation of an initial population, evaluation using a fitness function, selection, crossover, and mutation. This iterative process allows the algorithm to converge toward the optimal solution for a given problem. Genetic Algorithms serve as practical tools in solving multidisciplinary problems such as radome optimization. By considering structural and electromagnetic performance, GA can optimize design parameters — such as layer thicknesses and material properties — to efficiently solve complex, multi-objective problems where conventional optimization methods may struggle. This enhances both the transmission efficiency and structural durability of the radome. Figure 20 schematically illustrates the general workflow of the genetic algorithm. The process begins with the definition of the problem and the calculation of fitness values. The application of selection, crossover, and mutation operations follows this. A new generation is then created using the elitism method. The cycle continues until the stopping criterion is met.

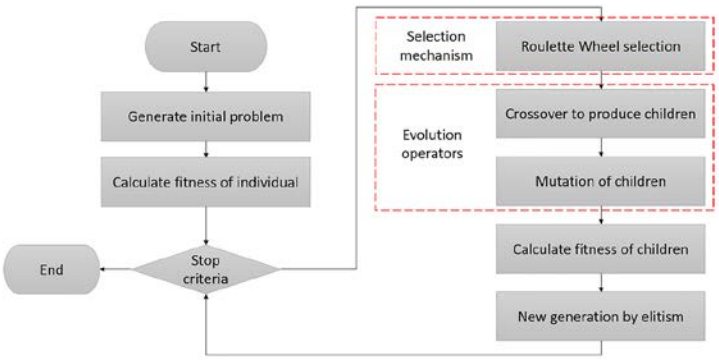

Figure 20. Suggested Flowchart for Genetic Algorithms [41]

Radome optimization using Genetic Algorithms employs mathematical models designed to optimize design variables such as layer thicknesses. For radome optimization, the objective function and constraints are formulated.

t_1, t_2, ..., t_n: thickness of each layer of the radome

Objective function:

$$Maksimize\ Tran = f(t_1, t_2, \dots, t_n)$$

Constraints:

$$\max(f_{i,j}) \leq f_{max}$$

$$t_{i,min} \leq t_i \leq t_{i,max}$$

5.2.1.3.2 Simulated annealing (SA) algorithm

The modeling and optimization of the performance of composite materials, depending on their formulations, manufacturing processes, and operating conditions, is one of the significant challenges encountered in developing new materials. The complexity of these interactions makes it difficult to establish analytical models. One of the methods used to optimize the performance of composite materials is the SA algorithm. This algorithm is a powerful approach for finding the global optimum in complex problems containing numerous local optima [42].

In the study conducted by M. Ananda Rao *et al.*, the SA algorithm was used to optimize multilayer composite plates [43]. In this study, a rapid optimization method was developed using the SA algorithm to maximize the fundamental natural frequency of multilayer composite plates. The analyses demonstrated that this approach is suitable and computationally efficient for the design of stiff fiber-reinforced plates. Furthermore, it was emphasized that the SA algorithm provides an effective solution for discrete variable optimization problems.

In the study by O. Erdal and F. O. Sonmez, the Simulated Annealing algorithm was applied to maximize the buckling load of composite laminates [44]. The Direct Simulated Annealing (DSA) algorithm successfully optimized the buckling load by taking the fiber orientations of each layer as design variables.

5.2.1.3.3 Particle swarm optimization (PSO)

Particle Swarm Optimization (PSO) is an optimization algorithm inspired by swarm behavior introduced in 1995 by Russell C. Eberhart and James Kennedy [45]. It has achieved significant success in various applications such as topology, shape, and size optimization and in solving many electromagnetic design problems [46], [47].

In the study conducted by Wanye Xu *et al.*, PSO was used to optimize BSE and transmission loss (TL) for radomes in aerial vehicles. The simulation results revealed that solutions optimized for BSE generally offered improved TL performance. The phenomenon of the TL wall was investigated within the objective function domain, and the study also demonstrated how the average angle of incidence changes as the antenna scans from the top to the bottom of the radome [48].

5.2.1.4 Gradient-based optimization

Gradient-based optimization methods are deterministic techniques widely used in engineering design problems to determine the direction of the search based on the objective function's derivative information (gradient). These methods gained popularity in the 1960s, particularly in the field of structural optimization, and were later adapted to aerodynamic and electromagnetic optimization problems [49]. Gradient-based search methods are iterative algorithms in which similar calculations are repeated at each iteration. The process begins from an initially selected design and progresses through successive improvements until the optimal solution is reached [50]. With subtypes such as steepest descent, conjugate gradient, and Quasi-Newton, these methods are effectively applied in parametric analyses and engineering problems requiring high precision. Figure 21 shows a gradient-based optimization curve. Starting from the designated initial design, the goal is to reach the minimum cost value through steps that progress in the direction of the gradient of the objective function. Each step is based on the derivative information of the cost function, and the process continues until convergence to the minimum point in the solution space.

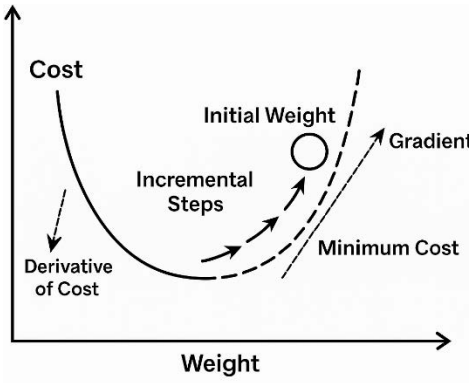

Figure 21. Optimization Using Gradients [51]

5.2.2 Multidisciplinary optimization software

Specialized software developed for the effective management of multidisciplinary optimization processes enables the simultaneous optimization of design parameters for each engineering discipline, allowing for the optimal balance of factors such as performance and cost.

In modern radome designs, the importance of the multidisciplinary optimization process has become even more evident. Radomes lie at the intersection of various engineering disciplines, including aerodynamics, electromagnetics, structural, and thermal analysis. Traditional designs in this field generally address each discipline separately, while modern approaches aim to optimize all disciplines together. This enables the development of more efficient, durable, and performance-oriented radome designs.

Advanced optimization software such as HEEDS, modeFRONTIER, COMSOL Multiphysics, and Altair HyperStudy significantly simplify multidisciplinary design processes with tools like parametric analysis, automated scenario management, and sensitivity analysis.

Altair HyperStudy stands out for its parametric optimization and structural analysis capabilities. This software allows the optimization of structural parameters such as material selection and thickness through FEM-based analyses while simultaneously evaluating RF transparency and mechanical durability to analyze the holistic performance of electromechanical systems.

COMSOL Multiphysics is an advanced finite element analysis software that integrates different physical disciplines in a single working environment, such as electromagnetics, structural, thermal, and fluid mechanics. In multidisciplinary engineering problems like radome design, the integrated analysis capabilities provided by this software enhance the design process's efficiency and accuracy. For the holistic evaluation of electromagnetic, structural, and thermal effects in radome design, RF, Structural Mechanics, and Heat Transfer modules within COMSOL Multiphysics are used together. The RF Module analyzes the transmission of electromagnetic waves through the radome at different frequencies, revealing the effects of material properties, particularly the dielectric constant (ε_r) and electrical conductivity (σ), on radar signal transmission. The Structural Mechanics Module calculates the mechanical responses of the radome under static and dynamic loads, allowing for the determination of parameters such as optimum thickness to maintain structural integrity. The Heat Transfer Module analyzes temperature distributions and resulting thermal stresses under environmental temperature conditions, enabling the assessment of thermal influences' effects on structural and electromagnetic performance.

Siemens HEEDS is software that automates optimization processes in engineering designs and provides AI-assisted analyses. Automated optimization processes allow engineers to find the optimal values of design parameters using HEEDS's advanced algorithms, rather than manually adjusting them. AI-assisted analysis makes the design process more efficient by leveraging machine learning capabilities in complex design problems. The trade-off analysis feature helps optimize multiple design objectives simultaneously and find the best balance between conflicting goals.

6. Radome Applications in Aerospace and Defense Industry

6.1 Usage In Military and Civilian Aircraft

Radomes are dome-shaped structures, typically made of composite materials, that protect radar systems in various applications such as communication, fire control, ground command systems, monitoring, missile guidance technologies, and radar systems on land and sea vehicles. Their primary purpose is to create a barrier between the antenna and the external environment, protecting external factors that could negatively affect the antenna's electrical performance. Radomes must resist wind, hail, snow, rain, icing, sand, lightning, temperature fluctuations, erosion, and aerodynamic forces. At the same time, they must be "invisible" to RF waves emitted by the antenna, ensuring the radar's ability to function fully [52]. The effectiveness of this function depends on the material components, shape design, application area, and the suitability of the radome for the frequency range. These structures are commonly used in terrestrial and marine communication systems, radar installations, and avionics system antennas on air platforms [53].

Radomes are used to protect various systems, including military and civilian radars, surveillance equipment, telecommunications, weather radar, coastal surveillance, satellite communications, microwave systems, broadcast equipment, as well as military and civilian flight simulators [54]. The geometry and dimensions of radomes are directly related to the antenna size and the application environment. In terrestrial applications, antennas are placed on fixed systems (such as ground stations and radars) or mobile platforms (such as land vehicles and sea vessels); on aircraft, antennas are typically integrated into the fuselages of civilian or military planes. Particularly in aircraft, the radome's weight, size, and shape are very important, as these platforms are subjected to significant environmental forces due to their high speeds. The radomes at the nose of large passenger aircraft and some military jets are typically more spherical and thicker. In contrast, supersonic jets prefer pointed nose cones to reduce the effects of shockwaves [55].

The shape of the radome is determined not only by the type of platform but also by the operation of the antenna. For example, sufficient space must be left inside to ensure a mechanically scanned antenna can scan smoothly without physical interference from the radome. In some applications, radomes are also a safety measure to prevent personnel from encountering the rotating antenna. Radomes provide external protection and must also be designed to minimize the impact on the antenna's electrical performance. Therefore, structures made from low-loss dielectric materials and typically with wall thicknesses corresponding to half the wavelength of the radio waves are preferred. The mechanical properties of radomes can vary greatly depending on the application; specifically, radomes designed for supersonic aircraft must meet much stricter weight and strength requirements than those used in ground systems. Shape, structural strength, and material selection are key factors in the design process [19].

6.1.1 Integration of radome with fighter aircraft, unmanned aerial vehicles (UAVs), and commercial aircraft

In military air platforms, particularly in fighter jets, radomes protect the radar systems integrated into the nose section and contribute to the aircraft's aerodynamic structure. For example, in modern fighter aircraft, active electronically scanned array (AESA) radar systems operate at high frequencies, and the radomes placed in front of these radars must be highly transparent and resistant to high temperatures. AESA radars are used for target detection, tracking, and missile guidance tasks.

In civilian aircraft, radomes are typically found as nose radomes. Commercial passenger aircraft are used to protect against weather radar systems and air traffic monitoring systems. These systems provide pilots with meteorological information such as storms, cloud structures,

and precipitation, enhancing flight safety. The accuracy of these systems is directly related to the electromagnetic transparency of the radome. Therefore, material selection, thickness, and shape design are crucial.

In applications such as missiles, which reach high speeds, are exposed to rapid temperature changes, experience high temperatures due to airflow, and must withstand external environmental factors, antennas are covered with radomes. In missiles, sensors at the nose or spiral and square patch antennas on the body are typically covered with radomes specifically designed to conform to the surface. These radomes protect the antenna and its electrical performance against the environmental challenges encountered during the mission [56].

In modern unmanned aerial vehicles (UAVs), radar systems play a critical role in tactical field surveillance and target tracking and are typically protected by radomes integrated into the aerodynamic structure. The KU-band radar system developed by Lincoln Laboratory and used on UAV platforms such as Amber (Figure 23) can detect low-altitude targets (e.g., helicopters and ground vehicles) at distances up to 15 km. Since the antenna structure rotates mechanically, the radome must also be designed to rotate with the antenna or be positioned to minimize the impact on the antenna aperture. Another factor to consider in radome design is the ability of the radar to operate in different modes (e.g., 360° wide-area scanning, sector scanning, target tracking, etc.) (Figure 22). This necessitates shaping the radome to maintain optical and structural transparency while covering the full range of antenna motion. Additionally, the UAV's flight at approximately 3 km altitude and its distance from enemy air defense systems increases the importance of stealth features. In this context, designing the radome to reduce RCS minimizes radar visibility and reduces the UAV's detection risk [57].

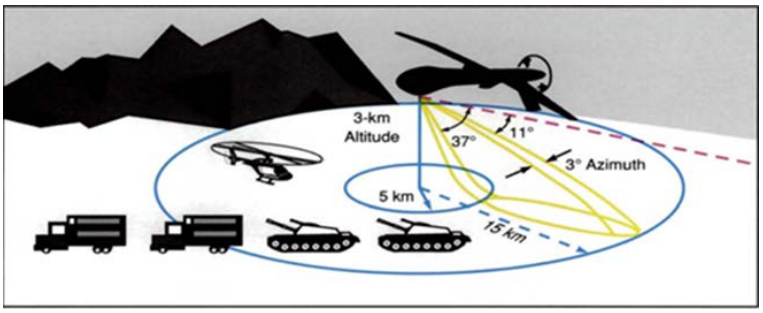

Figure 22. UAV monitoring and tracking zone with azimuth and elevation angles [57]

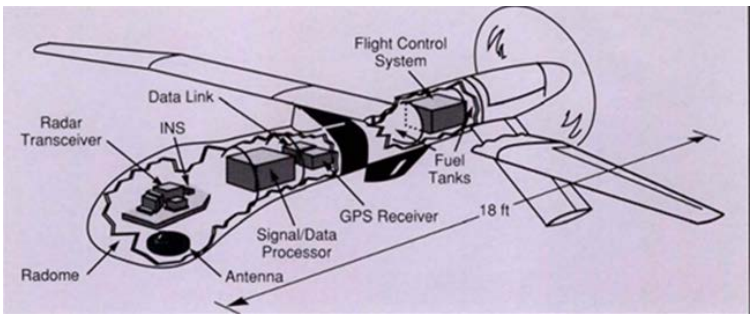

Figure 23. Components and arrangement of UAV systems [57]

The two main radomes commonly used in UAV systems are conformal radomes integrated into the fuselage and nacelle radomes placed externally in a capsule shape. Figure 24 shows a schematic of aerodynamic nacelle-shaped and teardrop-shaped radomes. Nacelle radomes, which are commonly preferred in Heron-type reconnaissance UAVs, stand out because they offer a wider scanning angle and minimally affect the structural design of the aircraft. However, the aerodynamic effects of these radomes and their integration with the structure must be carefully evaluated. Recent studies have shown that optimizing the radome shape along with the entire aircraft configuration effectively enhances radar performance while reducing drag [58]. A schematic of the Heron-type UAV and radar type is shown in Figure 25.

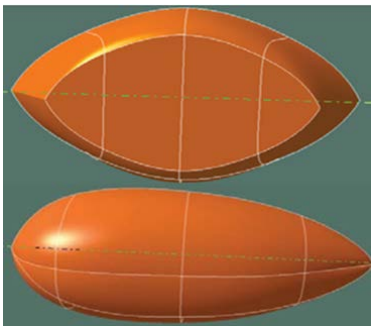

Figure 24. Examination of two radome shapes [58]

Figure 25. UAV and radar system, including antenna and parts [58]

6.1.2 Role in next-generation stealth technologies

Radomes play a critical role in next-generation stealth technologies. Commonly known as "stealth technology," low observability technology aims to conceal military vehicles, aircraft, ships, submarines, missiles, satellites, and ground vehicles from radar and infrared sensors. Stealth coating reduces RCS and makes it more difficult for aircraft to be detected. Stealth technology reduces radar reflections by using RAM and special geometries. While military aircraft use this technology to avoid radar detection, commercial airlines adopt certain elements to enhance safety and security. Stealth coatings reduce radar detection by either absorbing or redirecting radar signals. While military operations rely on this technology for confidentiality and security, civil aviation can also prevent hijacking events and detect unauthorized aircraft. Stealth technology is based on models that direct radar waves in specific directions. This makes it more difficult for the aircraft to be observed unless the radar receiver is positioned at a particular point relative to the aircraft as it moves. Radar receivers can detect any object or signal from a certain distance and convert this detection into a warning. This technique has been effectively used by military pilots for many years to track enemy aircraft, missiles, ships, submarines, satellites, and ground vehicles [59].

Since World War II, radar systems have been closely associated with aircraft radomes and low visibility (R&S) structures. Radar systems are used in various fields, from tracking enemy forces in the air and on the ground to weather observations [60]. Due to rapid advancements in radar technologies, enemy aircraft can now be detected earlier and with higher accuracy, which reduces the survival chances of friendly air platforms. As a result, designs with low radar cross-sections have become a priority in modern aircraft. RCS is a key parameter that indicates how easily an object can be detected by radar [61].

Low observability structures reduce the radar cross-section of platforms such as aircraft, spacecraft, cars, ships, tanks, and missiles. The mechanical strength of these structures, along with their response to broadband frequencies, is essential. Today, researchers are particularly focused on ideal radome structures with bandpass characteristics. These radomes reduce the RCS of the antenna outside the working frequency range while allowing electromagnetic signals to pass freely within the frequency range. Additionally, these structures must work appropriately for different incident angles and polarizations. The resonant frequency varies depending on the angle of incidence. Combining dielectric and metal surfaces can achieve designs with more stable resonant frequencies [60]. FSS technology is frequently used to enhance the penetration and survivability capabilities of airborne weapon platforms and reduce enemy detection, targeting, and interference capabilities. FSS structures are spatial filters designed as periodically arranged apertures on a conductive metal surface or as metal patches placed on a dielectric surface. The general system layout of an FSS-integrated radome, including the positioning of the FSS layer between the antenna and external environment, is shown in Figure 26a. The internal multilayered structure of the radome and its integration with dielectric layers are detailed in Figure 26b. The exploded view of a frequency-selective radome design, depicting the spatial arrangement of each component, is provided in Figure 27a. A closer view of the FSS layer, comprising periodic patch or aperture

elements responsible for frequency-selective behavior, is shown in Figure 27b. Integrating FSS into the radome wall, the radome becomes frequency-selective within a specific frequency band, thereby increasing the stealth of airborne platforms [62].

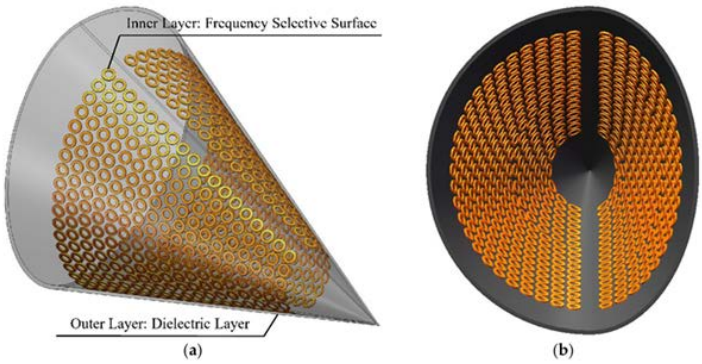

Figure 26. FSS integrated radome wall (a) general system layout; (b) internal structure of the radome [62]

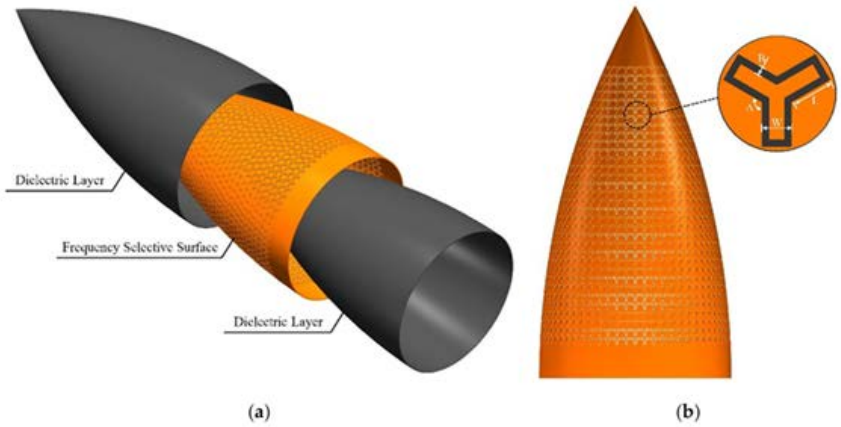

Figure 27. Frequency-selective radome design (a) exploded view; (b) FSS layer [62]

6.2 Radomes in Land and Naval Platforms

Radome use is not limited to air platforms. Radomes are also required for radar systems' secure and functional operation on land and sea platforms.

6.2.1 Radomes in land platforms

Radomes used on land and ship decks are typically designed in a truncated spherical shape or to be directly mounted on the ground. These stationary radomes are often coated with materials such as epoxy-based paints and reinforced with titanium dioxide additives to reduce the effects of ultraviolet radiation [52]. Examples of land radomes are shown in Figures 28 and 29.

Figure 28. Varieties of ground radome installations [52]

Figure 29. Ground-based radome at a naval installation [52]

Radomes protects antenna surfaces from environmental factors and provides security by concealing antenna systems from the public's view. Additionally, they prevent accidents that may occur from contact with rapidly rotating antennas. Figure 30 shows structures that serve as examples of such radome designs. Particularly for radar dishes, single-piece, large spherical dome-shaped radomes, typically of geodesic construction, protect rotating mechanisms and sensitive electronic components. In the case of rotating radar antennas, these structures ensure rotational stability and prevent wind-blown debris from damaging the antenna. Radomes also conceal the antenna's direction, making it impossible for external observers to detect which satellite or target the antenna is locked onto.

Figure 30. Radar radomes at a military or communication site [63]

It is believed that the Menwith Hill electronic surveillance station, reported to have over 30 radomes, periodically interferes with satellite communications. At Menwith Hill, radome protections contain additional measures to obscure the orientation of the antennas and, consequently, make it difficult to determine which satellites are being signaled. The radar system and surrounding radomes at Menwith Hill are shown in Figure 31.

Figure 31. Radar system at Menwith Hill [63]

A typical radome covers the parts of the antenna that are exposed to the external environment with weather-resistant, usually fiberglass-based composite materials, protecting them from debris, ice, and other adverse effects. From a structural load perspective, using radomes

significantly reduces the loads on the antenna, particularly in icy and windy conditions. Due to these advantages, the use of radomes is either mandatory or preferred in many tower-type systems.

6.2.2 Radomes in naval platforms

On marine platforms, particularly vehicles exposed to harsh environmental conditions such as warships and submarines, radomes designed to protect radar and communication systems are used. Radomes used on these platforms must be made from high-strength materials to withstand the corrosive effects of saltwater and changes in humidity and temperature. Additionally, the continuous motion on the sea — pitching, rolling, and yawing — may adversely affect the antenna's connection to the satellite, which is why radome systems designed to compensate for these movements are preferred. This way, even if the ship is in motion, the antenna can continuously track a fixed satellite, enabling uninterrupted data transmission. Large ships may use radomes with a diameter of 3 meters for wideband data transmission, while 26 cm diameter models are sufficient for smaller yachts [63].

The homogeneous wall structure, which constitutes approximately 90–96% of the radome surface, must be carefully designed from an electromagnetic performance perspective. A typical A-sandwich structure consists of three layers. The inner surface layer, foam core, and outer surface (hydrophobic coating). This structure allows electromagnetic waves to pass with minimal loss while providing high mechanical strength. Figure 32 illustrates how EM waves can be effectively transmitted through the radome layers of a foam core sandwich structure.

Figure 32. Antenna radome setup [53]

A structure in which a radome protects a parabolic antenna contributes to both enhancing performance and protecting against external environmental effects, particularly in underwater applications. The primary functions of radomes can be summarized as follows: First, they provide protection for the antenna and associated electronic equipment against the detrimental effects of environmental factors, thereby extending the system's overall lifespan. Second, radomes improve the antenna system's performance by ensuring more stable and reliable data transmission. Additionally, Fiber Reinforced Plastics' (FRP) radomes offer structural advantages due to their lightweight nature and economic feasibility. In submarine platforms, radomes play a critical role in ensuring the effective operation of antenna systems, even under high water pressure conditions.

Composite materials are preferred in naval and submarine platforms due to their advantages, such as high strength-to-weight ratio, ease of shaping, excellent electromagnetic interference (EMI) performance, and corrosion resistance. These properties are especially critical for submarine platforms that must leave minimal electromagnetic traces. In this context, E-glass and epoxy resin-based composite materials are commonly used in radome production due to their high permeability at microwave frequencies and good mechanical strength.

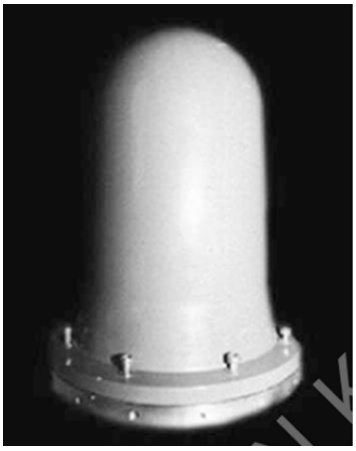

Figure 33. Submarine radome [53]

Structurally, submarine radomes consist of a flanged cylindrical body and a hemispherical dome and are usually mounted on the submarine platform using M6 bolts. Figure 33 shows a modular radome design assembled with mechanical fasteners. The outer surfaces of these sandwich-structured radomes are made from glass fiber reinforced plastic (GRP), while the inner parts are made from synthetic foam core. This design ensures the efficient transmission of electromagnetic waves, provides structural strength, and offers a safe, long-lasting, and high-performance solution for submarines and other marine platforms [53].

7. Conclusion

In conclusion, designing a radome is an engineering task that requires expertise from various disciplines, merging aspects of electromagnetic efficacy, structural strength, and aerodynamic performance. Choosing suitable materials, exceptionally lightweight composites with low dielectric properties and high mechanical durability, is crucial for achieving electromagnetic transparency and longevity. Innovative solutions such as metamaterials and FSS significantly enhance transmission efficiency, reduce radar cross-section, and provide adaptive functionalities. The choice of structural forms, whether monolithic or sandwich designs, offers specific advantages based on the intended mission, while the shape of the radome significantly influences drag and airflow characteristics during high-speed travel. Careful adjustment of layers' wall thickness, curvature, and orientation is vital for minimizing transmission losses and backscattering effects.

Advanced numerical techniques like FEM, FDTD, and MoM facilitate detailed electromagnetic assessments, while CFD is employed to analyze aerodynamics. These assessments are incorporated into multidisciplinary optimization frameworks supported by software such as HEEDS, modeFRONTIER, and COMSOL Multiphysics, which enhance the design workflow.

However, future investigations should address specific challenges, including the balance between electromagnetic transparency and structural strength, complexities associated with multilayer fabrication, environmental deterioration impact, and simulation findings validation under realistic operational scenarios.

The advancement of radome technology is focused on creating adaptive, lightweight, and high-efficiency designs that meet the rigorous standards of future aerospace systems. This is propelled by material innovations, optimization methodologies, and enhanced computational modeling.

Ethics committee approval and conflict of interest statement

This article does not require ethics committee approval.

This article has no conflicts of interest with any individual or institution.

Author Contribution Statement

Conceptualization, Mesut Uyaner (100%)

Literature review, Salman Murat Durukan (16%), Yeşim Öz (16%), Ahmet Kardaş (16%), Tuğba Burcu Çakır (16%), Ahmet İvenç (16%), Nursev Erdoğan (10%), Mustafa Kocaman (10%)

Writing, Salman Murat Durukan (20%), Yeşim Öz (20%), Ahmet Kardaş (20%), Tuğba Burcu Çakır (20%), Ahmet İvenç (20%)

Proofreading and review, Mesut Uyaner (100%)

References

[1] N. Khatavkar and B. K., "Composite materials for supersonic aircraft radomes with ameliorated radio frequency transmission-a review," *RSC Adv*, vol. 6, pp. 6709–6718, Dec. 2016, doi. 10.1039/C5RA18712E.

[2] S. Kumar and P. Gupta, "A review on ceramic and polymer materials for radome applications," in Proc. of the *2019 IEEE Indian Conference on Antennas and Propagation (InCAP)*, 19-22 December 2019, Ahmedabad, India [Online]. Available. IEEE Xplore, https.//ieeexplore.ieee.org. [Accessed. 20 Apr. 2025].

[3] E. Öziş, A. V. Osipov, and T. F. Eibert, "Metamaterials for microwave radomes and the concept of a metaradome. review of the literature," *Int J Antennas Propag*, vol. 2017, pp. 1–13, Jul. 2017, doi. 10.1155/2017/1356108.

[4] Ş. S. Fidan and R. Ünal, "A survey on ceramic radome failure types and the importance of defect determination," *Eng Fail Anal*, vol. 149, p. 107234, Jul. 2023, doi. 10.1016/j.engfailanal.2023.107234.

[5] F. Nazari, M. Taherkhani, M. Mokhtari, H. Aliakbarian, and O. Shekoofa, "Efficient design methodology for sandwich radome panels. a C-band design example," *IET Science, Measurement & Technology*, vol. 14, pp. 808–816, Sep. 2020, doi. 10.1049/iet-smt.2019.0209.

[6] M. Demirel, "Imparting non-flammability to glass fiber reinforced polyester composites (In Turkish)," M.S. thesis, Gazi Univ., Ankara, Türkiye, 2007.

[7] T. Sheret, C. Parini, and B. Allen, "Efficient design of a radome for minimised transmission loss," *IET Microwaves, Antennas & Propagation*, vol. 10, pp. 1662–1666, Jun. 2016, doi. 10.1049/iet-map.2016.0041.

[8] B. Audone, A. Delogu, and P. Mariondo, "Radome design and measurements," *IEEE Trans Instrum Meas*, vol. 37, pp. 292–295, Jun. 1988, doi. 10.1109/19.6069.

[9] G. A. Crowell Sr., "The descriptive geometry of nose cones," 1996. Accessed. Apr. 20, 2025. [Online]. Available. https.//web.archive.org/web/20110411143013/http.//www.if.sc.usp.br/~projetosulfos/artigos/NoseCone_EQN2.PDF

[10] B. Özdemir, E. Salamci, M. Kuloğlu, and A. M. Ateş, "Comparison of radome sandwich composite structures with finite element method," *Mater Today Proc*, vol. 34, pp. 297–303, Apr. 2020, doi. 10.1016/j.matpr.2020.03.800.

[11] F. Mazlumi and F. Mazlumi, "Analysis and design of flat asymmetrical a-sandwich radomes," *Journal of Telecommunication, Electronic and Computer Engineering*, vol. 10, pp. 9–13, Jul. 2018.

[12] Z. Wang, L. Tang, L. Zhou, Z. Jiang, Z. Liu, and Y. Liu, "Methodology to design variable-thickness streamlined radomes with graded dielectric multilayered wall," *IEEE Trans Antennas Propag*, vol. 69, pp. 8015–8020, Jun. 2021, doi. 10.1109/TAP.2021.3083799.

[13] K.A. Chepala, R.R. Ghali, J. Mukherjee, "Multilayer C-sandwich radome design for broad-band and multi-band airborne application" in Proc. of the *2021 2nd International Conference on Range Technology (ICORT)*, 5-6 August 2021, Chandipur, Balasore, India [Online]. Available. IEEE Xplore, https.//ieeexplore.ieee.org. [Accessed. 20 Apr. 2025].

[14] A. E. Fuhs, "Radar cross section lectures," Monterey, California, 1982.

[15] R. Shavit, *Radome electromagnetic theory and design*. Hoboken, NJ, USA. Wiley-IEEE Press, 2018.

[16] H. Uçar, "Radar cross section reduction," *Journal of Naval Science and Engineering*, vol. 9, pp. 72–87, 2013.

[17] Y. Ge, K. P. Esselle, and T. S. Bird, "A high-gain low-profile EBG resonator antenna," in Proc. of the *2007 IEEE Antennas and Propagation Society International Symposium*, 09-15 June 2007, Honolulu, HI, USA [Online]. Available. IEEE Xplore, https.//ieeexplore.ieee.org. [Accessed. 20 Apr. 2025].

[18] D. Peterson, J. Otto, and K. Douglas, "Radome boresight error and compensation techniques for electronically scanned arrays," in Proc. of the *Annual Interceptor Technology Conference*, Jun. 1993, Reston, Virginia [Online]. Available. https.//arc.aiaa.org. [Accessed. 20 Apr. 2025].

[19] D. D. Barnard, "Bore sight error analysis in seeker antennas. a fully functional GUI interfaced ray tracing solution," M.S. thesis, Stellenbosch Univ., Stellenbosch, South Africa, 2013.

[20] N. A. Korkut, A. Kara, and F. Ergün Yardım, "Conformal frequency selective surfaces in radome design. a mini review," *Savunma Bilimleri Dergisi*, vol. 20, pp. 211–222, Sep. 2024, doi. 10.17134/khosbd.1519500.

[21] E. Whalen, G. Gampala, K. Hunter, S. Mishra, and C. J. Reddy, "Aircraft radome characterization via multiphysics simulation," in Proc. of *2018 AMTA Proceedings*, 04-09 November 2018, Williamsburg, VA, USA [Online]. Available. IEEE Xplore, https.//ieeexplore.ieee.org. [Accessed. 20 Apr. 2025].

[22] R. U. Nair, M. Suprava, and R. M. Jha, "Graded dielectric inhomogeneous streamlined radome for airborne applications," *IET The Institution of Engineering and Technology*, vol. 51, pp. 862–863, May 2015, doi. 10.1049/el.2015.0462.

[23] J. L. Rotgerink, H. van der Ven, T. Voigt, E. Jehamy, M. Schick, and H. Schippers, "Modelling of effects of nose radomes on radar antenna performance," in Proc. of *2016 10th European Conference on Antennas and Propagation (EuCAP)*, 10-15 Apr. 2016, Davos, Switzerland [Online]. Available. IEEE Xplore, https.//ieeexplore.ieee.org. [Accessed. 20 Apr. 2025].

[24] B. M. Schroeder, "Electromagnetic and structural comparison of ultra-wideband antenna radomes," M.S. thesis, Kansas Univ., Lawrence, United States, 2020.

[25] C. M. S., P. G. K., R. G. D., S. S., and D. M., "Simulation of radome moving at supersonic speed," *IJSER International Journal of Scientific & Engineering Research*, vol. 11, pp. 197–206, Jun. 2020.

[26] A. S. Varma, S. G. Sathyanarayana, and S. J., "CFD analysis of various nose profiles," *International Journal of Aerospace and Mechanical Engineering*, vol. 3, pp. 26–29, Jun. 2016.

[27] L. de A. S. Carvalho and G. C. C. Filho, "CFD analysis of drag force for different nose cone design," in Proc. of *IX Fórum de Pesquisa e Inovação do Centro de Lançamento da Barreira do Inferno*, Oct. 2019, Natal, Rio Grande do Norte, Brazil [Online]. Available. ResearchGate, https.//www.researchgate.net [Accessed 21 Apr. 2025].

[28] J. D. Diaz, J. L. Salazar, A. Mancini, and J. G. Colom, "Radome design and experimental characterization of scattering and propagation properties for atmospheric radar applications," in Proc. of the *95th Annual Meeting of the American Meteorological Society. Atmospheric Radar Applications*, Jan. 2015, Phoenix, Arizona, USA [Online]. Available. ResearchGate, https.//www.researchgate.net [Accessed. 21 Apr. 2025].

[29] M. H. Bloom, D. Eisen, M. Epstein, L. Galovin, A. G. Hammitt, E. D. Kennedy, F. Lane, D. E. Magnus, A. A. Marino and H. S. Pergament, "Aerodynamic and structural analyses of radome shells,", General Applied Science Laboratories, USA, Feb. 1961.

[30] H. Ghasemnejad, H. Hadavinia, and A. Aboutorabi, "Effect of delamination failure in crashworthiness analysis of hybrid composite box structures," *Mater Des*, vol. 31, pp. 1105–1116, Mar. 2010, doi. 10.1016/j.matdes.2009.09.043.

[31] S. T. W. Lau, M. R. Said, and M. Y. Yaakob, "On the effect of geometrical designs and failure modes in composite axial crushing. a literature review," *Compos Struct*, vol. 94, pp. 803–812, Feb. 2012, doi. 10.1016/j.compstruct.2011.09.013.

[32] D. W. Wragg, Aviation Dictionary (In Turkish). Osprey, 1973.

[33] D. Davis, F. Mathew, J. K. P., N. Seenivasaraja, and K. A., "Design and analysis of different types of aircraft radome," in Proc. of the *National Conference on Recent Advancements and Innovations in Mechanical Engineering*, 2015, India [Online]. Available. https.//www.ijert.org

[34] M. T. Aamir, M. A. Nasir, Z. Iqbal, H. A. Khan, and Z. Muneer, "Multi-disciplinary optimization of hybrid composite radomes for enhanced performance," *Results in Engineering*, vol. 20, pp. 1–13, Oct. 2023, doi. 10.1016/j.rineng.2023.101547.

[35] X. Tang, W. Zhang, J. Zhu, F. L. Wang, and J. Lei, "Multidisciplinary optimization of airborne radome using genetic algorithm," in *Proc. of the 2009 International Conference on Artificial Intelligence and Computational Intelligence*, AICI 2009, H. Deng and L. Wang, Eds., Berlin, Heidelberg. Springer, 2009, pp. 150–158.

[36] "Multidisciplinary design optimization," Wikipedia, [Online]. Available. https.//en.wikipedia.org/wiki/Multidisciplinary_design_optimization [Accessed. 18 Apr. 2025].

[37] R. Ghadge, R. Ghorpade, and S. Joshi, "Multi-disciplinary design optimization of composite structures. a review," *Compos Struct*, vol. 280, pp. 1–7, Oct. 2021, doi. 10.1016/j.compstruct.2021.114875.

[38] H. Demirci and M. Kotan, "Recent metaheuristic algorithms used in the field of engineering (In Turkish)," in *Mühendislikte ileri ve çağdaş çalışmalar 1*, M. S. Cengiz, Ed., Kemeraltı-Konak, İzmir, 2023, ch. 11, pp. 176–196.

[39] E. V. Altay and O. Altay, "Comparison of current metaheuristic optimization algorithms with CEC2020 test functions (In Turkish)," *DUJE (Dicle University Journal of Engineering)*, vol. 12, pp. 729–741, Dec. 2021, doi. 10.24012/dumf.1051338.

[40] J. H. Holland, Adaptation in natural and artificial systems. United States of America. The MIT Press, 1992.

[41] R. P. E. Carrera, A. Pagani, and M. P. Lionetti, "MDO analysis of composite wing," M.S. thesis, Politecnico di Torino Univ., Turin, Italy, 2019.

[42] "What is simulated annealing?," Wikipedia, [Online]. Available. https.//en.wikipedia.org/wiki/Simulated_annealing [Accessed. 18 Apr. 2025].

[43] A. M. Rao, C. Ratnam, J. Srinivas, and A. Premkumar, "Optimum design of multilayer composite plates using simulated annealing," *Proceedings of the Institution of Mechanical Engineers, Part L. Journal of Materials. Design and Applications*, vol. 216, pp. 193–197, Jul. 2002, doi. 10.1177/146442070221600304.

[44] O. Erdal and F. O. Sonmez, "Optimum design of composite laminates for maximum buckling load capacity using simulated annealing," *Compos Struct*, vol. 71, pp. 45–52, Oct. 2004, doi. 10.1016/j.compstruct.2004.09.008.

[45] J. Kennedy and R. Eberhart, "Particle swarm optimization," in Proc. of the *ICNN'95 - International Conference on Neural Networks*, 27 November - 01 December 1995, Perth, WA, Australia [Online]. Available. IEEE Xplore, https.//ieeexplore.ieee.org. [Accessed. 20 Apr. 2025].

[46] J. Robinson and Y. Rahmat-Samii, "Particle swarm optimization in electromagnetics," *IEEE Trans. Antennas Propag.*, vol. 52, pp. 397–407, Feb. 2004, doi. 10.1109/TAP.2004.823969.

[47] G.-C. Luh, C.-Y. Lin, and Y.-S. Lin, "A binary particle swarm optimization for continuum structural topology optimization," *Appl Soft Comput*, vol. 11, pp. 2833–2844, Nov. 2011, doi. 10.1016/j.asoc.2010.11.013.

[48] W. Xu, B. Y. Duan, P. Li, N. Hu, and Y. Qiu, "Multiobjective particle swarm optimization of boresight error and transmission loss for airborne radomes," *IEEE Trans. Antennas Propag.*, vol. 62, pp. 5880–5885, Nov. 2014, doi. 10.1109/TAP.2014.2352361.

[49] R. Fletcher, Practical methods of optimization, Second. Scotland, UK. Wiley, 2000.

[50] J. S. Arora, Introduction to optimum design, Third. USA. Academic Press, 2012.

[51] "What is gradient based learning in deep learning?," JanBask Training. [Online]. Available. https.//www.janbasktraining.com/tutorials/what-is-gradient-based-learning-in-deep-learning/ [Accessed. 18 Apr. 2025].

[52] M. Ece, "Testing of small-sized radomes (In Turkish)," M.S. thesis, Erciyes Univ., Kayseri, Türkiye, 2006.

[53] N. V. Srinivasulu, S. Khan, and S. Jaikrishna, "Design and analysis of submarine radome," in Proc of the *International Conference on Research and Innovations in Mechanical Engineering. Lecture Notes in Mechanical Engineering*, S. S. Khangura, P. Singh, H. Singh, and G. S. Brar, Eds. New Delhi. Springer, Apr. 2014, pp. 11–26.

[54] V. M. Soumya, S. Navaneetha, A. N. Reddy, and J. Jagadesh Kumar, "Design considerations of radomes. A review," *International Journal of Mechanical Engineering and Technology (IJMET)*, vol. 8, pp. 42–48, Mar. 2017.

[55] H. U. Tahseen, L. Yang, and X. Zhou, "Design of FSS-antenna-radome system for airborne and ground applications," *IET Communications*, vol. 15, pp. 1691–1699, Mar. 2021, doi. 10.1049/cmu2.12181.

[56] O. Aktaş, "Design of a circularly polarized L1-band GPS/GNSS antenna with radome (In Turkish)," M.S. thesis, Hacettepe Univ., Ankara, Türkiye, 2019.

[57] C. E. Schwartz, T. G. Bryant, J. H. Cosgrove, G. B. Morse, and J. K. Noonan, "A radar for unmanned air vehicles," *The Lincoln Laboratory Journal*, vol. 3, pp. 119–143, 1990.

[58] W. Gan, J. Xiang, T. Ma, Q. Zhang, and D. Bie, "Low drag design of radome for unmanned aerial vehicle," in Proc. of the *2017 IEEE International Conference on Unmanned Systems (ICUS)*, 27-29 October 2017, Beijing, China [Online]. Available. IEEE Xplore, https.//ieeexplore.ieee.org. [Accessed. 20 Apr. 2025].

[59] N. Shirke, V. Ghase, and V. Jamdar, "Recent advances in stealth coating," *Polymer Bulletin*, vol. 81, pp. 9389–9418, Jul. 2024, doi. 10.1007/s00289-024-05166-4.

[60] R. Panwar and J. R. Lee, "Performance and non-destructive evaluation methods of airborne radome and stealth structures," *Meas Sci Technol*, vol. 29, pp. 1–29, Apr. 2018, doi. 10.1088/1361-6501/aaa8aa.

[61] H. Shin, D. Yoon, D. Y. Na, and Y. Park, "Analysis of radome cross section of an aircraft equipped with a FSS radome," *IEEE Access*, vol. 10, pp. 33704–33712, Mar. 2022, doi. 10.1109/ACCESS.2022.3162262.

[62] C. Qiu, S. Li, W. Zhang, L. Song, X. Li, Z. Yan, Y. Chen, and S. Suo, "A rapid modeling method for airborne FSS radomes based on dynamic customizable primitives," *Aerospace*, vol. 11, p. 505, Jun. 2024, doi. 10.3390/aerospace11070505.

[63] M. Wahab, "Radar radome and its design considerations," in Proc. of the *International Conference on Instrumentation, Communication, Information Technology, and Biomedical Engineering*, 23-25 November 2009, Bandung, Indonesia [Online]. Available. IEEE Xplore, https.//ieeexplore.ieee.org. [Accessed. 15 Apr. 2025].